

University of Minnesota
St. Anthony Falls Hydraulic Laboratory

Project Report No. 221

POTENTIAL FOR REDUCING KINETIC ENERGY LOSSES
IN LOW-HEAD HYDROPOWER INSTALLATIONS

by

Thomas Morel
Research Associate

Submitted to:

LEGISLATIVE COMMISSION ON MINNESOTA RESOURCES
STATE OF MINNESOTA
St. Paul, Minnesota

April, 1983

The University of Minnesota is committed to the policy that all persons shall have equal access to its programs, facilities, and employment without regard to race, creed, color, sex, national origin, or handicap.

TABLE OF CONTENTS

	<u>Page No.</u>
Abstract	iii
List of Symbols	iv
List of Figures	vi
I. INTRODUCTION	1
II. KINETIC ENERGY AT DRAFT TUBE INLET	5
III. CAVITATION CONSIDERATIONS	14
IV. DIFFUSER LITERATURE	20
A. Pressure Recovery in Diffusers	20
Definitions of Performance Coefficients	20
Uniform Flow with Boundary Layers	22
Effects of Turbulence	29
Distorted Inlet Profiles	31
Bent Diffusers	32
B. Effects of Swirl on Diffuser Flow	39
Definition of Swirl Ratio	39
Effects of Weak and Medium Swirl	43
Effect of Strong Swirl	53
Summary of Swirl Effects	56
C. Effect of Wall Jets on Diffuser Flow	59
Summary of Wall Jet Effects	64
D. Other Methods of Increasing Performance of Wide Angle Diffusers	68
V. IMPLICATIONS OF DIFFUSER LITERATURE FOR DRAFT TUBE DESIGN	69
Optimum Conical Diffusers	69
Distorted Velocity Profiles	70
Bent Draft Tubes	70
Swirl	70
Wall Jets	71

	<u>Page No.</u>
VI. SOME OBSERVATIONS ON DRAFT TUBE SIZE AND COST	73
A Note on Hydropower Codes	73
Draft Tube Area Ratio	73
Trends of Draft tube Size with Specific Speed ...	75
VII. SUMMARY AND RECOMMENDATIONS	78
A. Summary	78
B. Recommendations for Further Work	80
ACKNOWLEDGEMENT	81
REFERENCES	82

ABSTRACT

In order to reduce costs, low-head hydropower plants use turbines with increasingly higher specific speeds. A negative aspect of this trend is a resulting decrease in turbine efficiency. The present study addresses the issue of the kinetic energy of water leaving the runner and shows that at higher specific speeds it accounts for a large proportion of the available head. This places a special emphasis on the performance of draft tubes which must recover most of this energy in order to make high specific speed machines competitive on an economical basis. The study further reviews available diffuser literature. Several potentially attractive means for the development of highly efficient and compact draft tubes suitable for low-head (high specific speed) applications are suggested by the already published information. Finally, a number of areas are proposed where additional work is needed to achieve the above goal.

LIST OF SYMBOLS

A	area
AR	area ratio
B	blockage ratio, Eq. (34); height of blade passage
C_p	pressure coefficient, Eq. (25)
C_{p_α}	pressure coefficient, Eq. (26)
$C_{p_{\alpha\beta}}$	pressure coefficient, Eq. (18)
C_{p_e}	pressure coefficient, Eq. (28)
C_{p_i}	ideal pressure coefficient, Eq. (31)
C_{PRS}	pressure coefficient, Eq. (55)
C_{pr}	pressure coefficient, Eq. (58); Eq. (62)
c	jet mass flows/inlet mass flow
c_1	slot area/diffuser throat area
D	diameter
f	frequency
g	gravity
H	water head
k	jet velocity/main stream velocity
k.e.	kinetic energy at runner exit
L	length
M	momentum ratio, Eq. (36)
$m_{1,2}$	momentum parameters, Eq. (43) and (48)
N_s	dimensionless specific speed
p	static pressure
Q	volume flow rate
q	dynamic pressure
R	radius
t	wall thickness
U	velocity
u	velocity
V	velocity; volume
V_1	magnitude of total velocity vector at draft tube inlet

v_{a1}	axial velocity at drafttube inlet
v_{t1}	tangential velocity at draft tube inlet
W	width of a 2-D diffuser
z	elevation of turbine above tailwater level
α	kinetic energy factor, Eq. (3)
β	tangential kinetic energy factor, Eq. (3)
γ	specific mass
δ^*	displacement thickness
δ	swirl angle, Eq. (39)
η	efficiency
λ	profile distortion parameter, Eq. (35)
λ_1, λ_2	loss coefficients, Eq. (32), (33)
ϕ	tipspeed coefficient; diffuser half-angle
ρ	density
σ	cavitation number
σ_{TC}	Thoma's sigma
Ω	angular momentum, Eq. (43)
ω	angular velocity

Subscripts

a	atmosphere; axial
c	centerline
j	jet
t	tangential
v	vapor
w	wall
z	axial
1	draft tube inlet
2	draft tube exit
θ	tangential

LIST OF FIGURES

Figure No.

- 1a Vertical Kaplan Turbine.
- 1b Tube Turbine.
- 1c Rim Turbine.
- 1d Bulb Turbine.
- 2 Speed coefficient based on turbine exit diameter D_t .
(Adapted from Arndt et al., 1983.)
- 3 Speed coefficient based on wheel inlet diameter for Francis turbines and a turbine exit diameter for Kaplan turbines. (Adapted from Daugherty and Francini, 1977.)
- 4 Curves of best efficiency obtained by the three turbine types plotted versus specific speed (from Arndt et al., 1983).
- 5 Ratio N_s/ϕ obtained from several sources: — Daugherty and Franzini (1977), —•— Arndt et al. (1983), --- de Siervo and de Leva (1978).
- 6 Dimensionless average axial velocity at runner exit for Kaplan turbines. (Adapted from de Siervo and de Leva, 1978.)
- 7 Definition sketch for net head (from Arndt et al., 1983).
- 8 Cavitation index as a function of specific speed; — Arndt et al. (1983), --- de Siervo and de Leva (1978).
- 9 Performance chart for conical diffusers, $B_1 = 0.02$, based on data from Cockrell and Markland (1963). (Adapted from Sovran and Klomp, 1965).
- 10 Performance chart for conical diffusers obtained by replotting data from Fig. 9 in different coordinates.

Figure No.

- 11 Performance data for conical diffusers. (Adapted for McDonald and Fox, 1966.)
 - a) Contours of pressure recovery in terms of spreading angle.
 - b) Contours of effectiveness in terms of spreading angle.
 - c) Contours of pressure recovery in terms of area ratio.
 - d) Lines of first appreciable stall (a-a) and of maximum pressure recovery at constant length (α - α).
— conical diffusers, --- two-dimensional diffusers.
 - e) Same as d) but plotted in terms of area ratio.
- 12 Optimum diffuser geometries for prescribed dimensionless diffuser length. (Adapted from Klein, 1981.)
- 13 Maximum pressure recovery at $AR = 5$ and $B_1 = 0.02$.
- 14 Effects of inlet blockage on the performance of diffusers with an area ratio $AR = 5$. (Adapted from Klein, 1981.)
- 15 Lines of first appreciable stall for non-uniform (wake-like) inlet profiles. (Adapted from Kaiser and McDonald, 1980.)
- 16 Comparison of measured pressure recovery of two-dimensional diffusers with wake-like inlet profile (data points) and uniform inlet profile (lines). \square --- $L/W_1 = 3$, \circ --- $L/W_1 = 6$, ∇ --- $L/W_1 = 12$. C_{p1} is the ideal, inviscid, pressure coefficient. (Adapted from Wolf and Johnston, 1969.)
- 17 Comparison of pressure recovery for three different inlet conditions: (a) uniform profile, (b) splitter plate wake profile, (c) rod wake profile. $L/W_1 = 3.0$. (Adapted from Waitman et al., 1961).
- 18 Location of first appreciable stall (line a-a) as a function of turning angle in curved diffusers with circular arc centerline and linear area distribution. Line p-p denotes maxima of individual curves. (Adapted from Fox and Kline, 1962).
- 19 Performance of circular-arc designs of curved diffusers at first-stall limits for $\Delta\beta = 50^\circ$, contrasted to performance of straight wall diffusers at their first-stall limits. (Adapted from Sagi and Johnston, 1967.)
- 20 Comparison of typical curved diffuser shapes for $\Delta\beta = 70^\circ$, obtained by an inverse design procedure, to circular-arc shape (denoted by ---). (Adapted from Sagi and Johnston, 1967).

Figure No.

- 21 Performance comparison of straight wall, circular-arc and inverse-design shape diffusers. In all cases the inverse designs lie in-between the straight wall and the circular arc diffusers. (Adapted from Sagi and Johnston, 1967.)
a) $L/W_1 = 4$, $\Delta\beta = 70^\circ$
b) $L/W_1 = 6$, $\Delta\beta = 70^\circ$
c) $L/W_1 = 10$, $AR = 1.6$
d) $L/W_1 = 10$, $AR = 2.0$
- 22 Typical design of a swirling flow generator producing Rankine vortex-type distribution. (Adapted from Neve and Thakker, 1981).
- 23 Diffuser performance coefficient as a function of area ratio. Shaded area covers cone spreading angles in the range $2\phi = 4^\circ-15.8^\circ$, symbols show results for $2\phi = 31.2^\circ$. (Adapted from McDonald et al., 1971.)
a) Axial inlet flow.
b) Swirling inlet flow, highest swirl ($\delta = 18.4^\circ$).
- 24 Pressure recovery coefficients as a function of swirl angle at $AR = 4$. (Adapted from Senoo et al, 1978.)
- 25a Effect of swirl on static pressure coefficient C_p at $AR = 4$. Diffuser is followed by a tailpipe. (Adapted from Neve and Wirasinghe, 1978.)
- 25b Effect of swirl on kinetic energy factor α along the diffuser length. (Adapted from Neve and Wirasinghe, 1978.)
- 26 Pressure coefficient $C_{p\alpha\beta}$ extracted from data in Figs. 24 and 25.
- 27 Ratio of pressure coefficient for swirling case to pressure coefficient for non-swirling case for $AR=4$. (Adapted from Neve and Thakker, 1981.)
- 28 Lines of critical swirl rates for onset of flow reversal at tube exit and for fully developed surge. (Adapted from Cassidy, 1969.)

Figure No.

- 29 Flow regimes with swirling flow in divergent conduits. (Adapted from Falvey, 1971).
Regime 1 - Weak swirling flow, laminar throughout. No surging.
Regime 2 - A disturbance forms on axis. Flow laminar throughout. Surges.
Regime 3 - Laminar flow upstream from disturbance, turbulent downstream. No surging.
Regime 4 - Turbulent throughout. No surging.
Regime 5 - Stall on centerline of conduit. Turbulent throughout. Surge irregular.
Regime 6 - Stall extends throughout conduit. Flow entirely turbulent. Surge is regular when stall region is small, irregular when stall region is large.
- 30 Surge frequency as a function of momentum parameter for a straight tube. (Adapted from Cassidy and Falvey, 1970.)
- 31 Amplitude of pressure pulses during surging. (Adapted from Falvey and Cassidy, 1970.)
- 32 Surging frequencies for straight cylinders and diffusing passages. (Adapted from Falvey and Cassidy, 1970.)
- 33 Effect of wall jet injection velocity on the performance of diffusers with $AR = 3$. (Adapted from Nicoll and Ramaprian, 1970.)
a) $2\phi = 10^\circ$
b) $2\phi = 20^\circ$
c) $2\phi = 30^\circ$
- 34 Effect of wall jet mass flow injection rate on the performance of two-dimensional diffusers with a fixed wall length $L/W_1 = 4.25$. (Adapted from Fiedler and Gessner, 1972.)
a) $2\phi = 14^\circ$
b) $2\phi = 20^\circ$
c) $2\phi = 30^\circ$
- 35 Effect of slot size on the maximum effective diffuser pressure recovery. (Adapted from Fiedler and Gessner, 1972.)
- 36 Effects of wall jet injection velocity, mass flow rate and momentum ratio on pressure recovery coefficient. Axial injection and 30° cone angle. (Adapted from Duggins et al., 1978.)
- 37 Effect of momentum ratio on pressure recovery coefficient for tangential injection and 30° cone angle. (Adapted from Duggins et al., 1978.)

Figure No.

- 38 Comparison of axial and tangential injections for two slot sizes. — axial, --- tangential. (Adapted from Duggins et al., 1978.)
- 39 Water Velocity at draft tube inlet for Kaplan turbines. (Adapted from de Siervo and de Leva, 1978.)

POTENTIAL FOR REDUCING KINETIC ENERGY LOSSES
IN LOW-HEAD HYDROPOWER INSTALLATIONS

I. INTRODUCTION

Low-head hydropower plants are typically equipped with axial machines with fairly high specific speeds, with values reaching four and more in non-dimensional terms. In these installations the initial cost of equipment is an important consideration, and there is a continuing interest in increasing further the specific speed of the machines in order to reduce their size and cost. A negative aspect of the trend toward higher and higher specific speed machines is the associated decrease in turbine efficiency which is due to the increasing portion of the net head which still remains as kinetic energy of the water at the runner exit.

The draft tubes of water turbines have a dual function. One is to enable the setting of the turbine above the tailwater level without losing any head, which is accomplished by maintaining an uninterrupted water column between the runner exit and the tailwater. The other function is to recover a part of the kinetic energy of the water leaving the machine, and convert it into additional potential energy available to the turbine.

For purposes of evaluation of plant efficiency, the draft tubes are considered to be integral parts of the water turbines, and their efficiency is lumped into the total hydraulic efficiency of the turbine/draft tube assembly. This is done in recognition of the fact that the draft tube design depends very strongly on the turbine configuration, to which its shape has to conform.

The various turbine configurations applied to low-head water power applications include vertical Kaplan turbine (Fig. 1a), tubular turbine (Fig. 1b), rim-generator turbine (Fig. 1c), and the bulb turbine (Fig. 1d). Of these, the first type calls for a draft tube incorporating a 90 degree bend, the second requires an S-shaped draft tube, while the last two permit a straight draft tube design. In addition, the turbine can influence the draft tube design through limitations posed by cavitation considerations, requiring a certain elevation with respect to the tailwater and thus a particular path the water must follow.

The draft tube shape is also influenced by the needs of the particular hydropower site, which might be an existing structure that is being updated. All of this leads to a situation in which no two draft tubes are alike and each needs an individual design. This is not much of an issue for a large power plant where model studies are routine, but for small low

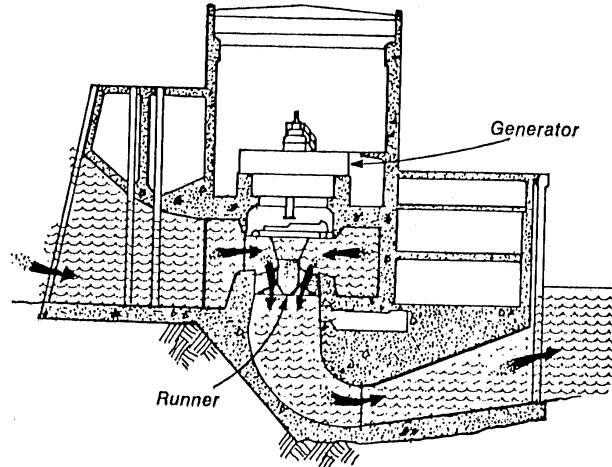


Fig. 1a. Vertical Kaplan Turbine.
(from Carlson & Samuelson, 1978)

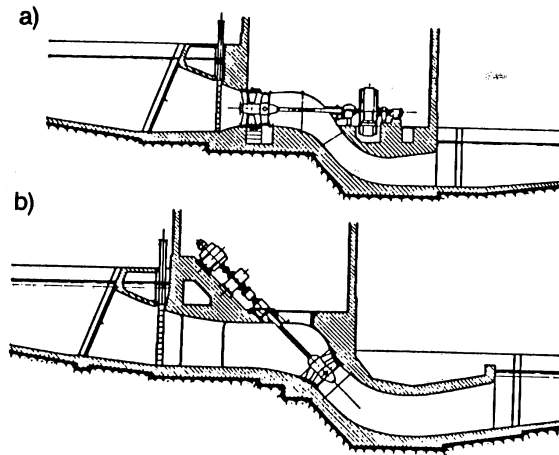


Fig. 1b. Tube Turbine.
(from Arndt et al., 1983)

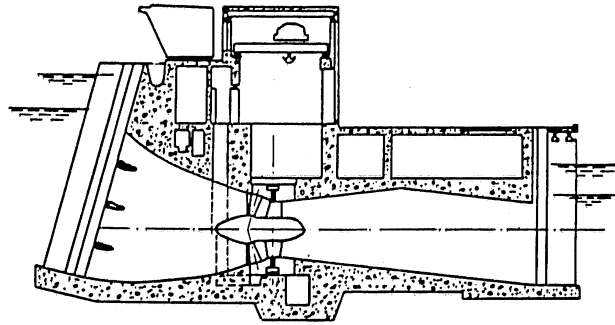


Fig. 1c. Rim Turbine.
(from Arndt et al., 1983)

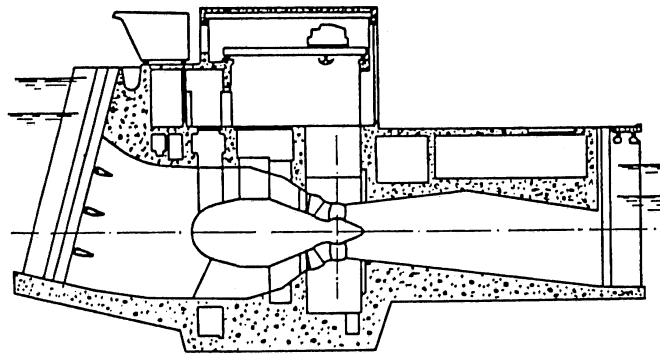


Fig. 1d. Bulb Turbine.
(from Arndt et al., 1983)

head powerplants the economics of the project often does not allow for sufficient model studies and refinements. Yet, it is especially important for low-head powerplants to have correctly designed draft tubes. This is because these plants use high speed machines where the potential for large losses in draft tubes is the greatest.

One of the objectives of this study was to quantify the proportion of the net head which remains in the form of kinetic energy at the runner exit, and express it in terms of standard turbine dimensionless parameters. A part of this energy is lost in the draft tube and at its exit; therefore, the next objective was to evaluate the potential for reducing these losses. To this end, the report reviews available diffuser literature to determine what is known about diffusers in general, including optimum area ratio and wall angle, the effects of inlet flow non-uniformity, effects of diffuser curvature (bends), the beneficial influence of flow swirl, and improvements in performance by injection of wall jets.

II. KINETIC ENERGY AT DRAFT TUBE INLET

The kinetic energy at the throat of the draft tube (exit from the runner) may be expressed as a fraction of the net head as

$$\frac{\text{k.e.}}{H} = \frac{\int V_1^2 v_{a1} dA}{2g H Q} \quad (1)$$

where V_1 is the magnitude of the total velocity vector at the throat and v_{a1} is the axial velocity component. The flow rate Q is given by

$$Q = \int v_{a1} dA = \bar{v}_{a1} A_1 \quad (2)$$

The integral in Eq. (1) may be evaluated as

$$\int v_{a1}^3 dA + \int v_{t1}^2 v_{a1} dA = \bar{v}_{a1}^3 A_1 (\alpha_1 + \beta_1) \quad (3)$$

where v_{a1} and v_{t1} are the axial and tangential velocity components, respectively, α_1 and β_1 represent augmentation of the actual kinetic energy over the kinetic energy associated with the mean axial velocity \bar{v}_{a1} ; α_1 represents augmentation due to axial velocity non-uniformity ($\alpha \geq 1$) and β_1 represents the kinetic energy in the tangential velocity component. Thus we can write

$$\frac{\text{k.e.}}{H} = (\alpha_1 + \beta_1) \frac{\bar{v}_{a1}^2}{2gH} = (\alpha_1 + \beta_1) \frac{(Q/A_1)^2}{2gH} \quad (4)$$

This expression may be used to calculate the kinetic energy at the throat of any particular reaction machine.

If one wishes to analyze this ratio for groups of machines described in terms of standard dimensionless turbine parameters, one may manipulate Eq. (4) further. One may eliminate the flow rate Q using the specific speed

$$N_s = \frac{\omega \sqrt{\text{power}/\rho}}{(gH)^{5/4}} = \sqrt{\eta} \frac{\omega \sqrt{Q}}{(gH)^{3/4}} \quad (5)$$

or

$$Q = \frac{1}{\eta} (N_s/\omega)^2 (gH)^{3/2} \quad (6)$$

which yields

$$\frac{\text{k.e.}}{H} = \frac{\alpha_1 + \beta_1}{\eta^2} \frac{2}{\pi^2} \left(\frac{N_s \sqrt{2gH}}{\omega D_1} \right)^4 \quad (7)$$

and if the value of the tip speed coefficient ϕ

$$\phi \equiv \frac{1}{2} \omega D_1 / \sqrt{2gH} \quad (8)$$

is available, then one can substitute it to obtain

$$\boxed{\frac{\text{k.e.}}{H} = \frac{\alpha_1 + \beta_1}{\eta^2} \frac{1}{8\pi^2} \left(\frac{N_s}{\phi} \right)^4} \quad (9)$$

In order to use this expression we need as an input N_s based on power, ϕ based on throat diameter D_1 , efficiency η and some educated guesses on α_1 and β_1 .

The efficiency data may be obtained from Fig. 4, taken from Arndt et al. (1983), Fig. 28.

Using data collected in Fig. 2 (which is a plot of Moody's data taken from Arndt et al., Fig. 26) and Fig. 3 [from Daugherty and Franzini (1977), Fig. 16.15] one can derive the ratio N_s/ϕ as presented in Fig. 5. The two sources agree for the Francis turbine^s, but the Kaplan turbine data from the two sources show two different trend lines, which intersect in the region of interest.

Based on a survey of 130 existing Kaplan turbines, de Siervo and de Leva (1978) deduced a variation of the average axial velocity at the draft tube inlet with specific speed (Fig. 6). This variation may be represented by a linear function

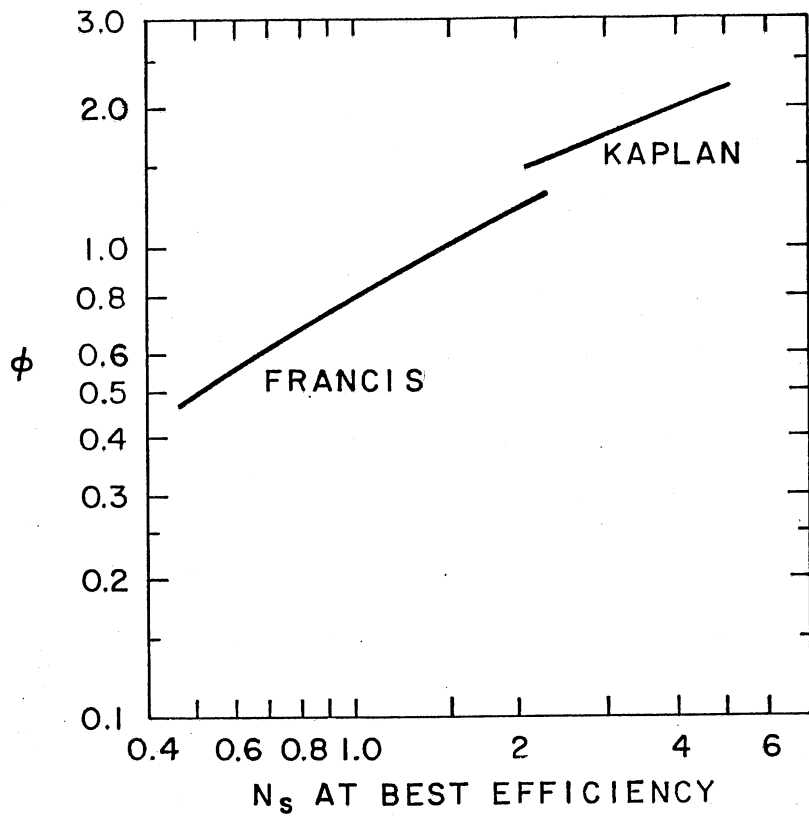


Fig. 2. Speed coefficient based on turbine exit diameter D_t .
 (Adapted from Arndt et al., 1983.)

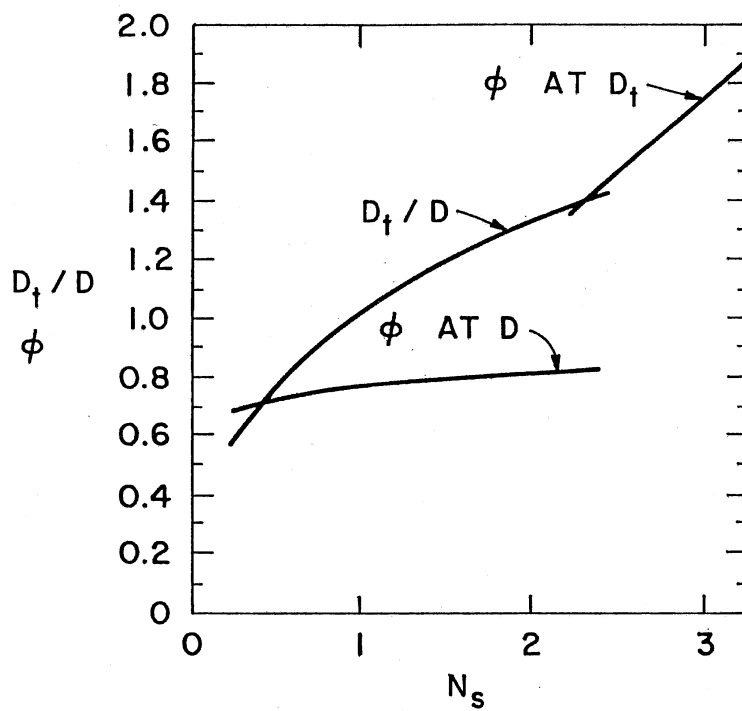


Fig. 3. Speed coefficient based on wheel inlet diameter for Francis turbines and a turbine exit diameter for Kaplan turbines. (Adapted from Daugherty and Francini, 1977.)

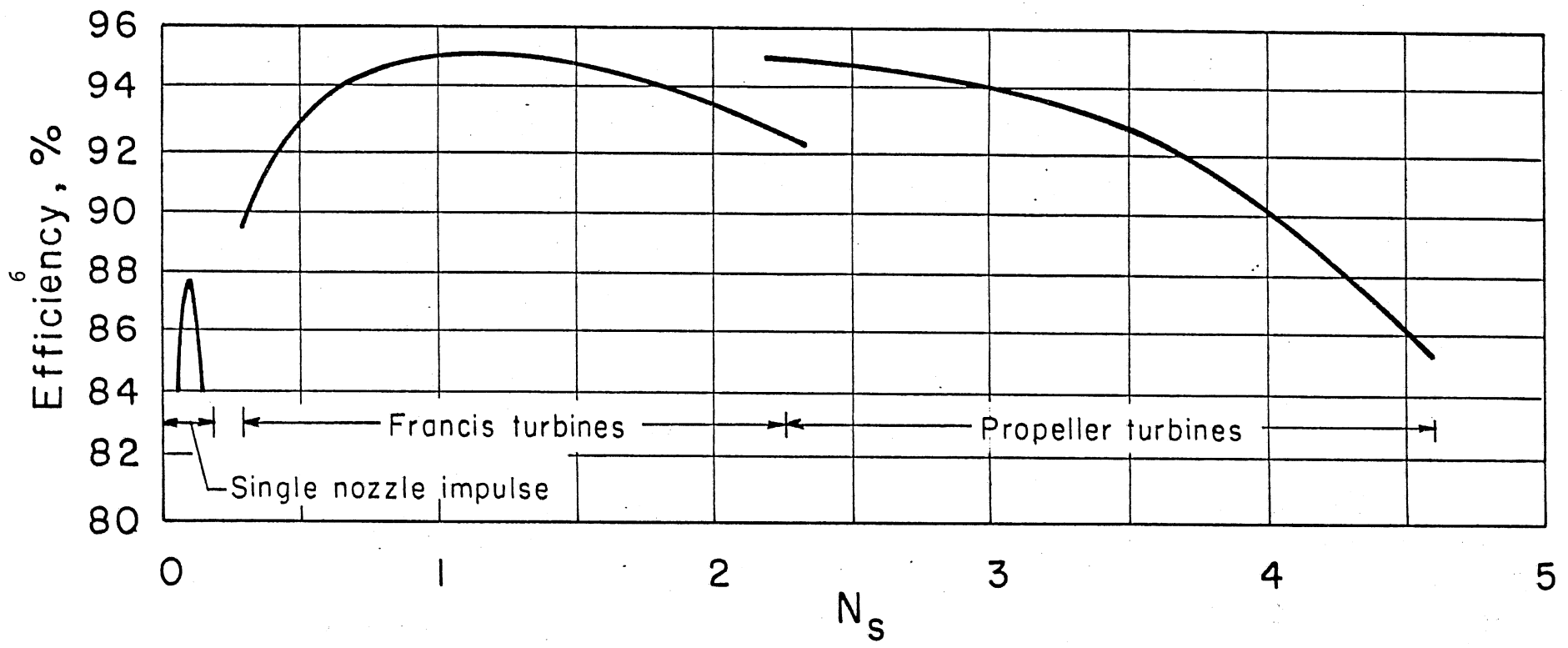


Fig. 4. Curves of best efficiency obtained by the three turbine types plotted versus specific speed (from Arndt et al., 1983).

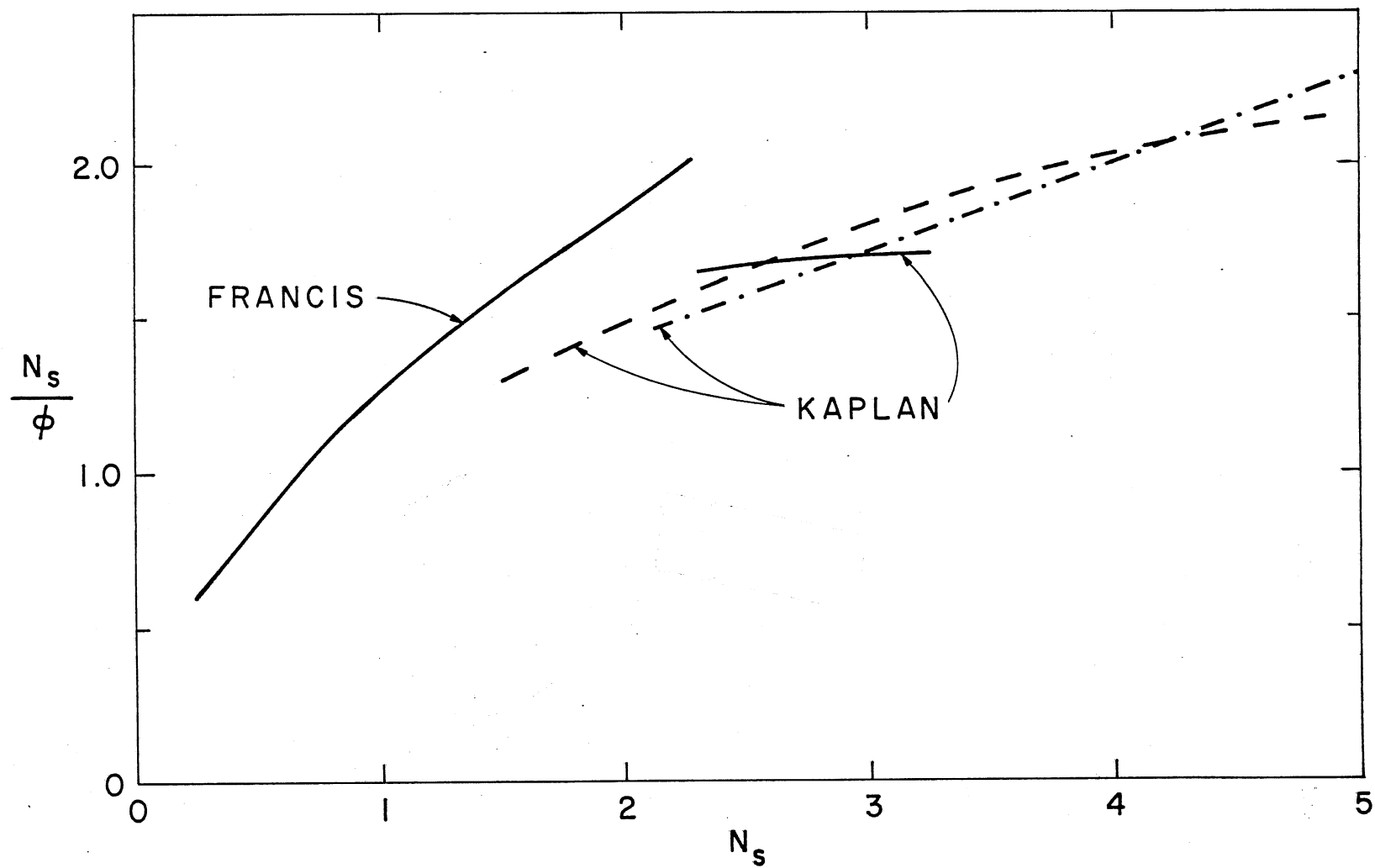


Fig. 5. Ratio N_s/ϕ obtained from several sources: — Daugherty and Franzini (1977),
— • — Arndt et al. (1983), --- de Siervo and de Leva (1978).

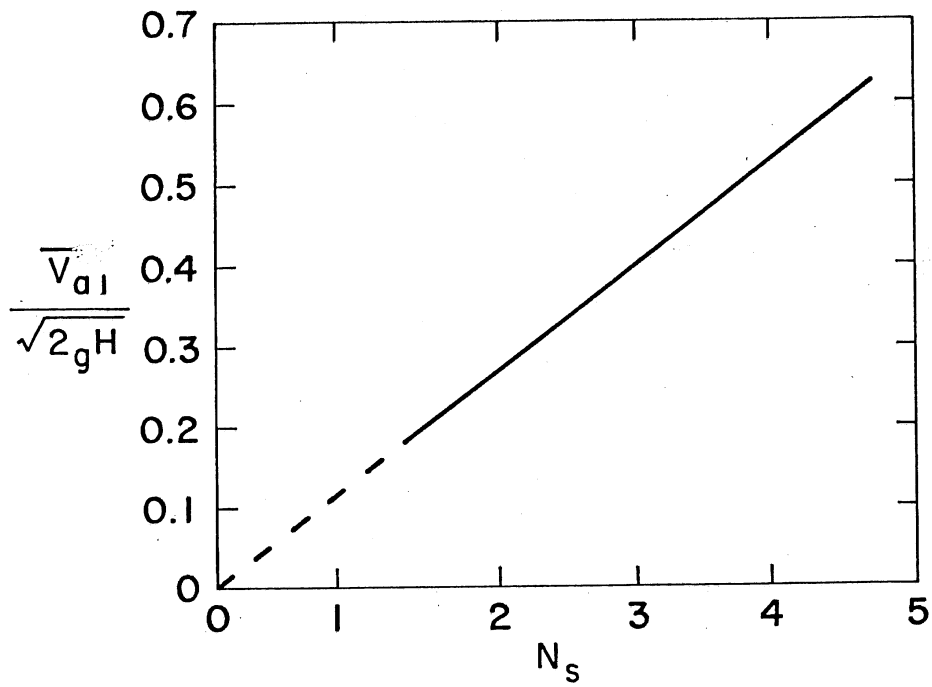


Fig. 6. Dimensionless average axial velocity at runner exit for Kaplan turbines. (Adapted from de Siervo and de Leva, 1978.)

$$\boxed{\frac{\bar{v}_{a1}}{\sqrt{2gH}} = 0.13 N_s} \quad (10)$$

Substituting Eq. (10) into Eq. (4) gives a particularly simple expression for kinetic energy (k.e.)

$$\boxed{\frac{\text{k.e.}}{H} = 0.0169 (\alpha_1 + \beta_1) N_s^2} \quad (11)$$

The ratio $\bar{v}_{a1}/(2gH)^{1/2}$ may be also obtained from Eq. (4) and (9) from which it follows that

$$\frac{\bar{v}_{a1}}{\sqrt{2gH}} = \frac{1}{\eta \sqrt{8} \pi} \left(\frac{N_s}{\phi} \right)^2 \quad (12a)$$

Equating both expressions we in effect deduce the dependence of N_s/ϕ on N_s of the machines de Siervo and de Leva's surveyed. This dependence has the following form:

$$\frac{N_s}{\phi} = 1.07 \eta^{1/2} N_s^{1/2} \quad (12b)$$

Using the data for efficiency from Fig. 4, one can plot Eq. (12b) into Fig. 5. It is seen that Eq. (12) agrees quite well with the curve obtained from Moody's data. It is of interest to note that Fig. 5 shows that the ratio N_s/ϕ at comparable values of N_s is lower for Kaplan turbines than for Francis turbines. This agrees with the finding of de Siervo and de Leva (1978), that for the same head and rating Kaplan turbines are larger and have a smaller water velocity.

Using Eq. (11) and assuming a value of $\alpha_1 = 1.5$ and $\beta_1 = 0.0$ (no residual swirl) one can make an estimate of the kinetic energy at the draft tube throat. Taking a high speed axial machine with $N_s = 4$ one obtains

$$\frac{\text{k.e.}}{H} = 0.0169 \times 1.5 \times 16 = 0.41$$

This means that at $N = 4$, 41 percent of the available potential energy exits the turbine in^s the form of kinetic energy. This is a very large fraction, which increases further with the square of N_s . It is clear that for high speed machines, it is imperative to provide very well designed draft tubes recovering the maximum of this energy in order to maintain the efficiency of the whole system at an acceptable level.

In the remainder of this report we shall refer frequently to the relations established in this section. In particular, use will be made repeatably of Eq. (10), obtained from de Siervo and de Leva, which gives a simple linear relationship between \bar{v}_{a1} and N_s . It should be realized, however, that looking at Fig. 5 one could make an argument for a little different exponent for (N_s/ϕ) vs. N_s which would lead through Eq. (12a) to a slightly different relationship between \bar{v}_{a1} and N_s .

III. CAVITATION CONSIDERATIONS

One of the constraints in hydropower installations is cavitation in the turbine. Cavitation has to be avoided because it causes damaging pitting, produces flow instability and mechanical vibrations, and it also reduces the efficiency of the plant. The cavitation occurs first at the point of minimum pressure, usually near the trailing edge on the suction side of the runner blades.

The criterion for avoidance of cavitation is usually characterized by a cavitation number called Thoma's sigma, defined as

$$\sigma_T = \frac{(p_a/\gamma - z) - p_v/\gamma}{H} > \sigma_{TC} \quad (13)$$

where z is the elevation at the turbine blades above the tailwater level (Fig. 7). Equation (13) simply states that the turbine (here we mean a matched turbine-draft-tube assembly) will cavitate when $(p_a/\gamma - z)$ drops low enough for $\sigma_T = \sigma_{TC}$, or if the available head increases enough to bring about the equality $\sigma_T = \sigma_{TC}$.

The determination of the parameter σ_{TC} is done by model testing of the proposed plant, and it should represent the maximum value found during operation over the entire range of operating conditions (especially at high flows and low heads). The resulting value of σ_{TC} is found to be a very strong function of the turbine specific speed, as shown in Fig. 8, which may be approximated by

$$\sigma_{TC} \approx 0.12 N_s^{1.61} \quad (\text{Francis}) \quad (14a)$$

$$\sigma_{TC} = 0.079 N_s^{1.81} \quad (\text{Kaplan}) \quad (14b)$$

The up-to-date surveys of de Siervo and de Leva (1976, 1978) give correlations with about the same values of σ_{TC} but with a smaller exponent of N_s

$$\sigma_{TC} \approx 0.10 N_s^{1.41} \quad (\text{Francis}) \quad (15a)$$

$$\sigma_{TC} \approx 0.11 N_s^{1.46} \quad (\text{Kaplan}) \quad (15b)$$

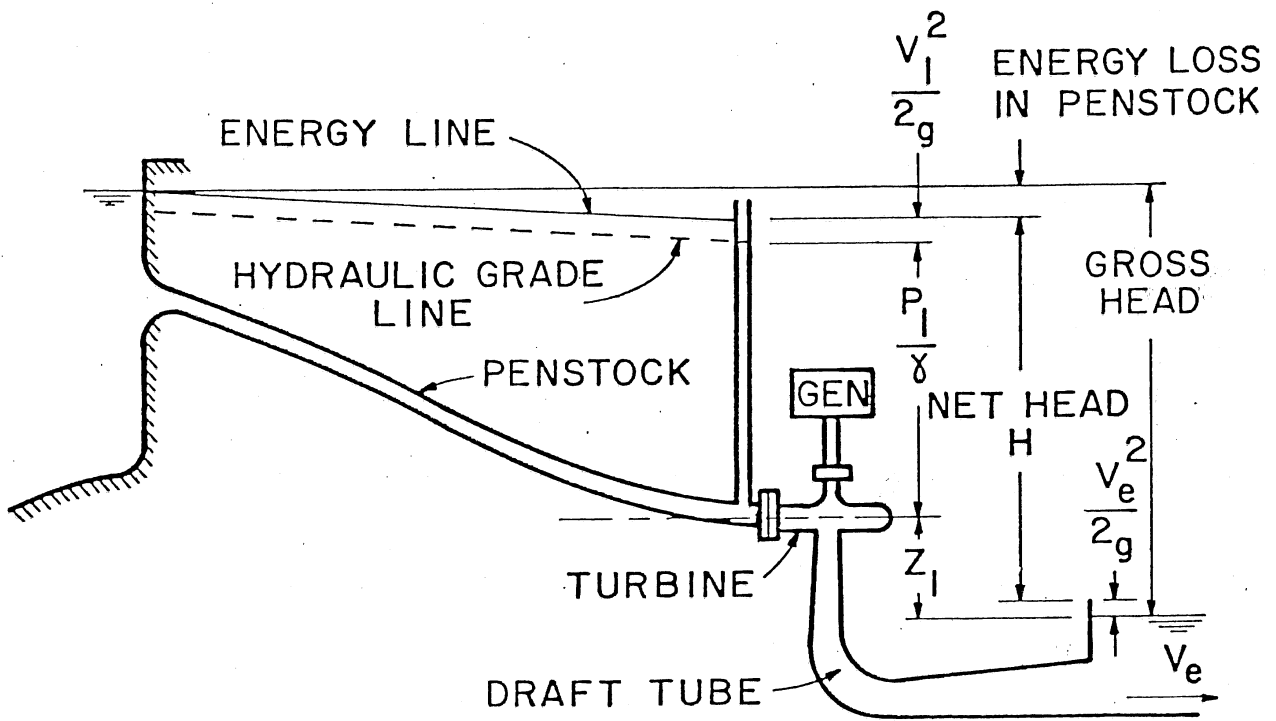


Fig. 7. Definition sketch for net head (from Arndt et al., 1983).

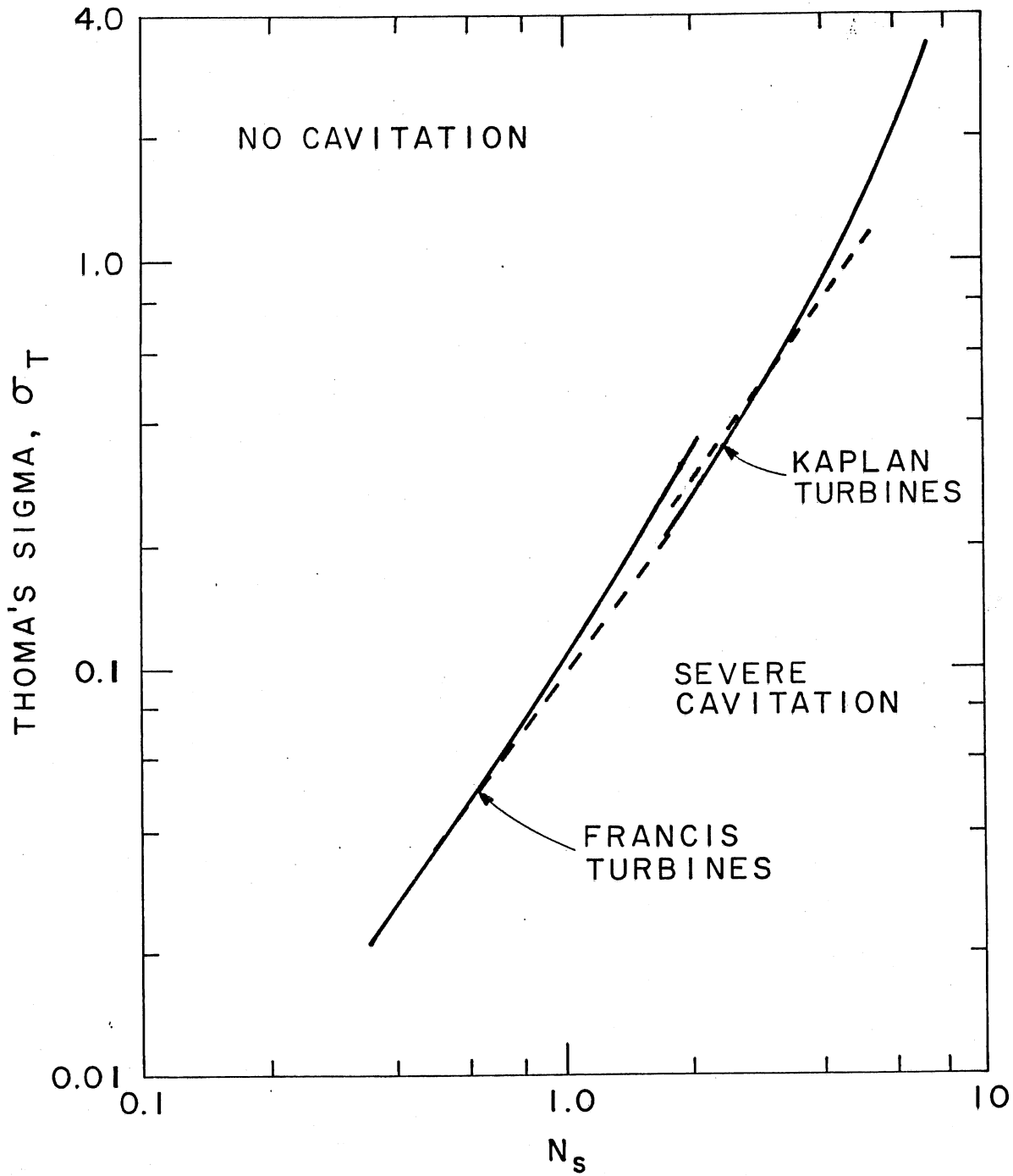


Fig. 8. Cavitation index as a function of specific speed; —Arndt et al. (1983), ---de Siervo and de Leva (1978).

The main use of Thoma's sigma is for the determination of the maximum allowable draft head permitting cavitation-free operation of the plant:

$$z_{\max} = (p_a - p_v)/\gamma - \sigma_{TC}H \quad (16)$$

The first term on the right-hand side is on the order of 10 meters at sea level conditions, giving a fair leeway for construction of the draft tube. However, the second term can be of comparable magnitude, especially at high specific speeds at which σ_{TC} rises rapidly. The resulting value of z_{\max} may then be quite small or even negative, giving rise to substantial excavation and civil works costs.

The kinetic energy at the throat of the draft tube, and its recovery in the draft tube, both have an effect on the value of σ_{TC} , which is worth exploring. Let us start with the conditions at the runner exit, where

$$P_1 = p_a - \gamma z - \gamma C_{p_{\alpha\beta}} \text{ (k.e.)} \quad (17)$$

where

$$C_{p_{\alpha\beta}} \equiv \frac{\Delta p}{(\alpha_1 + \beta_1)q} \equiv \frac{C_p}{\alpha_1 + \beta_1} \quad (18)$$

Cavitation will appear in the machine when the cavitation number based on the runner tip speed exceeds a critical value. This may be expressed as

$$\frac{P_1 - p_v}{1/2\rho V_{t1}^2} > \sigma_{\text{crit}} = -C_{p_{\min}} \quad (19)$$

where $C_{p_{\min}}$ is the pressure minimum on the runner blades. Substituting Eq. (17) into (19) we obtain

$$\frac{(p_a - \gamma z) - p_v}{\gamma H} > \sigma_{\text{crit}} \phi^2 + C_{p_{\alpha\beta}} \left(\frac{\text{k.e.}}{H} \right) \quad (20)$$

Comparing Eq. (20) to Eq. (13) we find that

$$\sigma_{TC} = \sigma_{crit} \phi^2 + C_{p_{\alpha\beta}} \left(\frac{k.e.}{H} \right) \quad (21)$$

Equation (21) shows that the conventionally defined σ_{TC} is in fact composed of two contributions: one is a cavitation number directly related to the pressure minimum on the runner blades, and the second one has to do with the additional lowering of the pressure at the runner exit due to the pressure recovery in the draft tube.

From the survey of de Siervo and de Leva (1977, 1978) for Kaplan turbines we find

$$\phi \approx 0.94 N_s^{1/2} \quad (\text{Kaplan}) \quad (22)$$

As for the exit kinetic energy, combining Eqs. (4) and (10) we obtain

$$\frac{k.e.}{H} = (\alpha_1 + \beta_1) 0.017 N_s^2 \quad (23)$$

Substituting Eq. (22) and (23) into Eq. (21), leads to

$$\sigma_{TC} = 0.88(-C_{p_{min}})N_s + 0.017 C_{p_{\alpha\beta}} (\alpha_1 + \beta_1) N_s^2 \quad (24)$$

The parameters α_1 , β_1 , and $C_{p_{\alpha\beta}}$ may be assumed to be fairly independent of N_s . However, $(-C_{p_{min}})$ tends to increase with specific speed because of increased blade setting angle. Consequently, the first contribution to Thoma's sigma, the cavitation number, increase faster than linearly with N_s . The second term, the kinetic energy contribution, increases even faster with a quadratic dependence, and it becomes important at high specific speeds. These trends account for the observed sharp rise in σ_{TC} (Fig. 8).

To illustrate the effect of the kinetic energy term on the draft head z_{max} , let us evaluate its contribution for $N_s = 4$, $C_{p_{\alpha\beta}} = 0.7$ and $(\alpha_1 + \beta_1) = 1.5$. Substituting these values, one obtains $\sigma_{ke} = 0.29$. The total σ_{TC} calculated from Eq. (14b) has a value of 0.97, while Eq. (15b) gives 0.83. It follows that 30 - 35 percent of the total σ_{TC} at $N_s = 4$ is due to the additional lowering of pressure caused by high water velocity at the runner exit.

It may be seen from Eq. (24) that increasing both the kinetic energy at the throat, k.e./H, and the diffuser efficiency has an adverse effect on

the maximum permissible elevation z_{\max} . Paradoxically then, improving the draft tube efficiency can have an indirect adverse effect on the plant cost, and this should be taken into account in the overall cost/benefit assessment.

IV. DIFFUSER LITERATURE

In the course of this study available literature dealing with laboratory diffuser experiments was reviewed to provide some guidance to optimum diffuser design and to general trends of diffuser performance with key geometrical parameters. The Reynolds numbers used in these experiments were typically on the order of 10^5 , which is much lower than in hydropower applications. It is usually assumed that the nature of diffuser flows (qualitatively speaking) is Reynolds number independent, once it is high enough for transition phenomena to be absent inside the diffuser ($Re_D > 100,000$ has been suggested). Nevertheless, the performance may be expected to be a function of Reynolds number (albeit weak) through its effects on boundary layer resistance to separation. The performance might be expected to improve as Reynolds number increases.

A. Pressure Recovery in Diffusers

The performance of a diffuser depends on its geometry and on the details of the inlet flow. The key geometrical parameters of straight-walled conical diffusers are the spreading angle, length to diameter ratio, and, if applicable, also the length of a constant area tailpipe attached to the diffuser exit. The tailpipe often improves the performance of wider-angle diffusers, but in the following we shall concentrate on data taken in diffusers without tailpipes, as they are more relevant to draft tubes.

In this section we shall discuss separately pressure recovery in diffusers with inlet flow which are essentially uniform except for wall boundary layers, distorted inlet flows, effects of turbulence and also the effects of bends on diffuser performance. Before we start, however, we shall review the coefficients commonly used to describe diffuser performance.

Definitions of Performance Coefficients

The performance may be defined in a variety of ways, the most commonly used being the pressure coefficient

$$C_p \equiv \frac{p_2 - p_1}{\frac{1}{2} \rho \bar{U}_1^2} = \frac{\Delta p}{q_1} \quad (25)$$

where \bar{U}_1 is the spatially averaged inlet velocity. Other definitions consider the non-uniformity of the inlet velocity profile which enhances the inlet kinetic energy

$$C_{p\alpha} \equiv \frac{\Delta p}{\alpha_1 \bar{q}_1} \quad (26)$$

where

$$\bar{q}_1 \equiv \int_{A_1} \frac{1}{2} \rho u_1^3 dA / (A \bar{U}_1) \quad (27)$$

This pressure coefficient is always smaller than C_p , but for undistorted turbulent entry flow α_1 is close to unity, reaching a maximum value of 1.06 for a fully developed turbulent pipe.

Cockrell (1964) proposes "efficiency" defined as

$$C_{pe} \equiv 1 - \frac{\int_{A_2} (p + \frac{1}{2} \rho u^2) u dA - \int_{A_1} (p + \frac{1}{2} \rho u^2) u dA}{\int_{A_1} \frac{1}{2} \rho u^3 dA} \quad (28)$$

which may be written as

$$C_{pe} \equiv \frac{\Delta p}{\alpha_1 \bar{q}_1} + \frac{\alpha_2}{\alpha_1} \left(\frac{A_1}{A_2} \right)^2 \quad (29)$$

that considers the exit kinetic energy represented by the second term not as a loss, but as energy which is still available.

Another type of efficiency that is often used is

$$\eta \equiv C_p / C_{p_i} \quad (30)$$

where

$$C_{p_i} \equiv 1 - \frac{1}{AR^2} \quad (31)$$

is the ideal pressure rise coefficient for an inviscid flow with a uniform inlet profile.

One other type of definition is the loss coefficient alternately defined as

$$\lambda_1 = 1 - C_p \quad (32)$$

or

$$\lambda_2 = 1 - C_p / [1 - (A_1/A_2)^2] = 1 - C_p/C_{p_i} \quad (33)$$

For most practical applications the definition $C_{p\alpha}$ is the most appropriate one to use, as it indicates the efficiency with which the kinetic energy available at the diffuser inlet is converted into a pressure rise.

Uniform Flow with Boundary Layers

This type of inlet flow is the most-widely studied, covering the range from very thin boundary layers to a fully developed pipe flow. For boundary layer inlet flows the most accepted conical diffuser data seem to be those of Cockrell and Markland (1963) as presented by Sovran and Klomp (1965); see Fig. 9. The figure shows lines of constant pressure coefficient C_p , and also a line of optimum pressure recovery C_p^* for a prescribed L/D_1 , as well as a line of optimum recovery C_p^{**} for a prescribed area ratio AR. Figure 10 presents the same data redrawn in linear coordinates. These figures show that the best recovery coefficient is obtained with a very mild diffuser with a spreading angle $2\phi \approx 6^\circ$, and with area ratios up to six.

Another similar set of results was obtained in a detailed study by McDonald and Fox (1966). Their results are summarized in Figs. 11a - 11e. Figure 11a shows that conical diffusers perform the best (at a fixed L/D_1) for core angles not too different from 8° , with higher angles for short diffusers and vice versa. The figure also shows that for any given angle, the performance continues to improve monotonically with diffuser length at least up to $L/D_1 = 16$. Figure 11b shows the same results plotted in terms of effectiveness $\eta \equiv C_p/C_{p_i}$, revealing that if the kinetic energy leaving the diffuser is considered not lost but still available further downstream, then the best cone angle is close to 5° . The lines of first appreciable stall and C_p^* are presented in Figs. 11d and 11e, showing that maximum pressure recovery at fixed L/D_1 is achieved when there is some limited stall present. The figures also include the equivalent lines for 2-D diffusers.

A comprehensive set of data for conical diffusers was compiled by Klein (1981), who included a range of inlet blockage ratios defined as

$$B_1 = \frac{4\delta^*}{D_1} = 1 - \frac{\bar{U}}{U_c} \quad (34)$$

This data is summarized in Fig. 12 which shows lines of C_p^* at various inlet blockage ratios. The effect of increasing blockage ratio is to shift the optimum line to lower spreading angles.

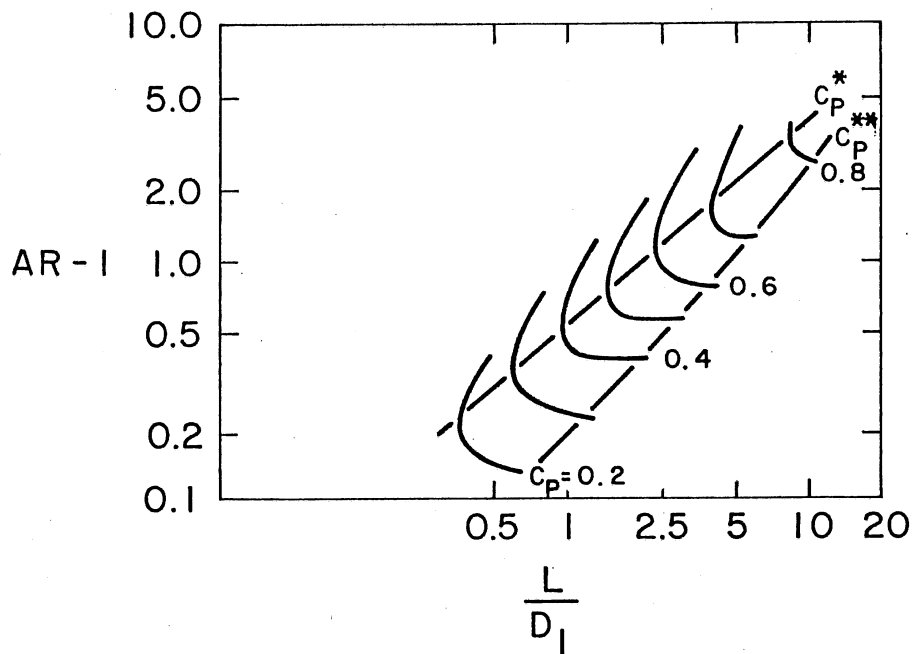


Fig. 9. Performance chart for conical diffusers, $B_1 = 0.02$, based on data from Cockrell and Markland (1963). (Adapted from Sovran and Klomp, 1965).

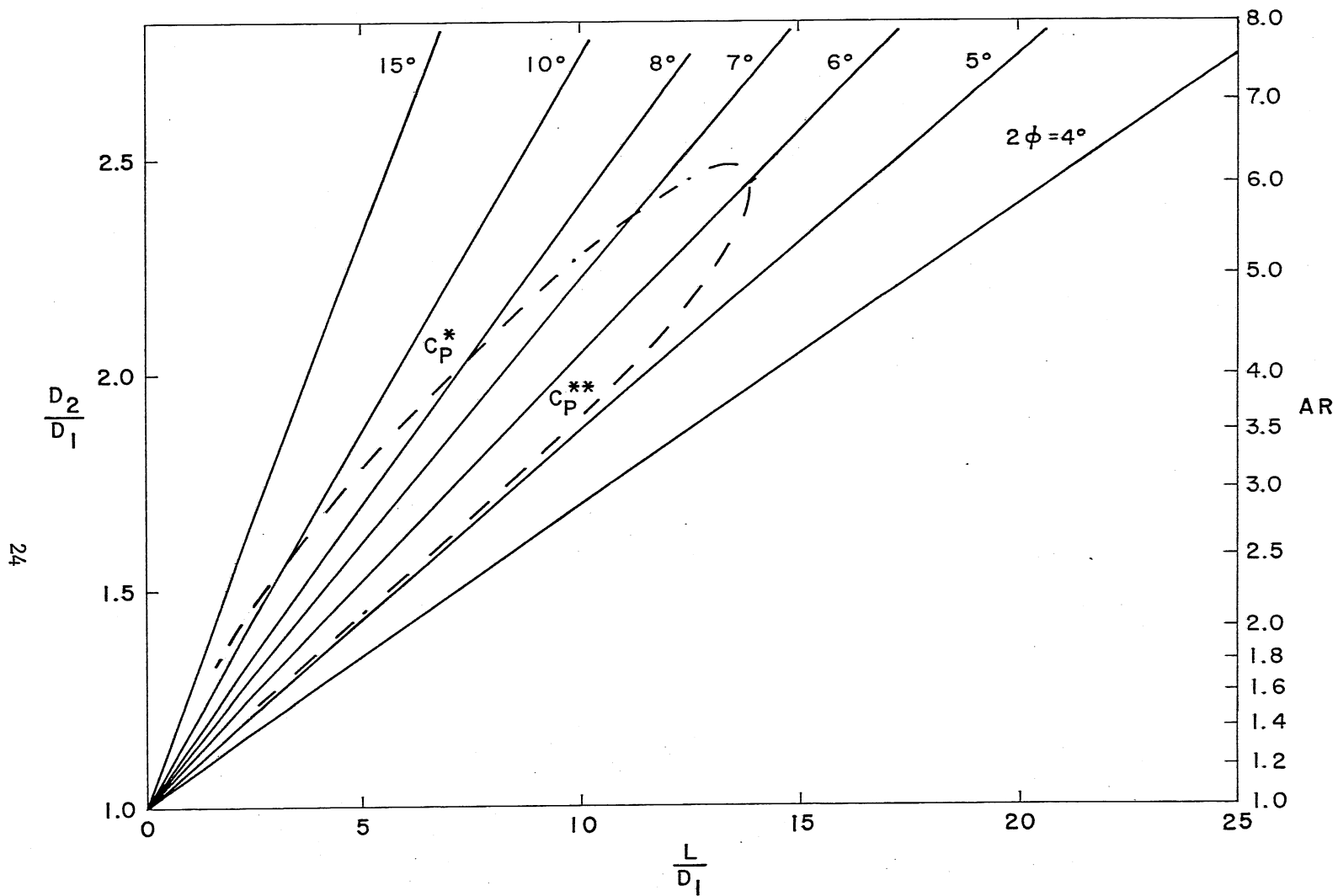
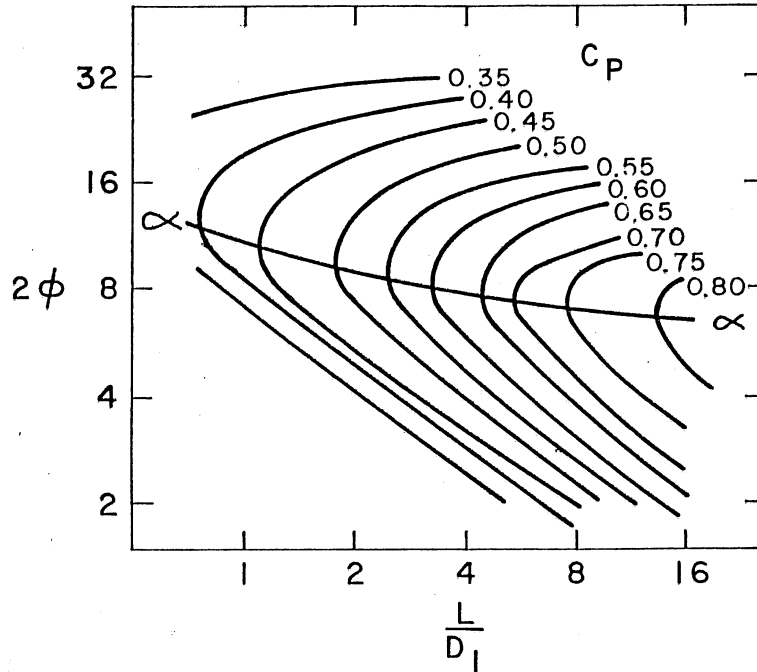
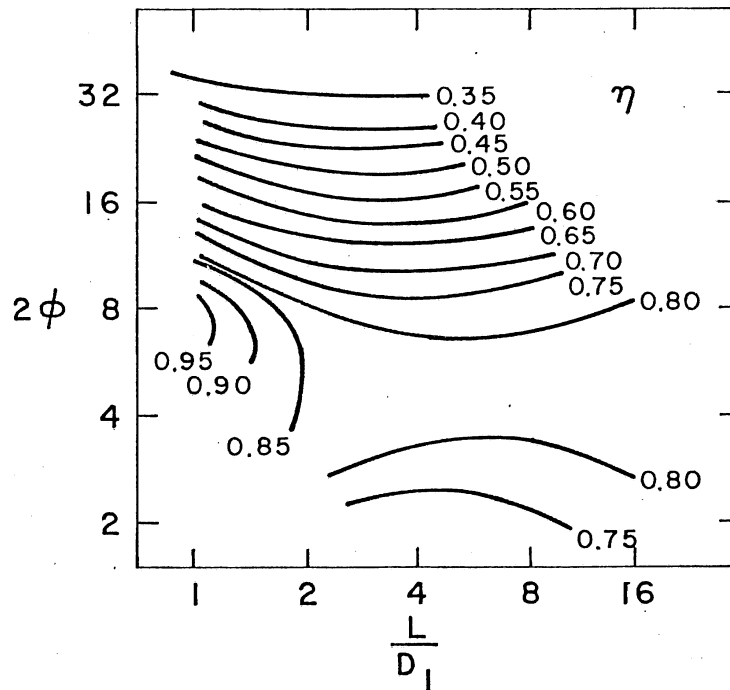


Fig. 10 . Performance chart for conical diffusers obtained by replotting data from Fig. 9 in different coordinates.

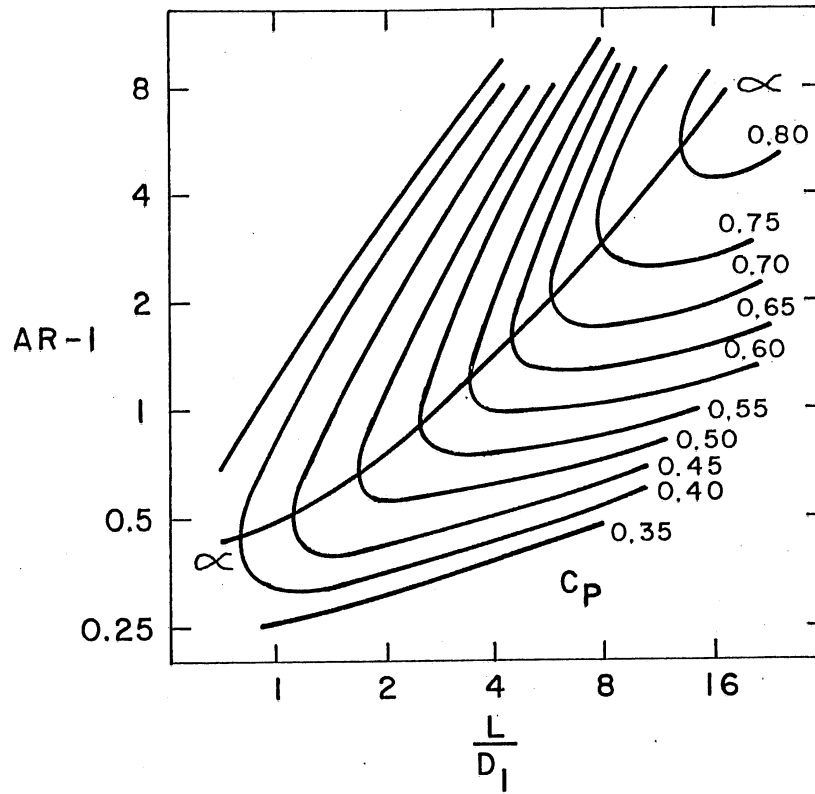


a) Contours of pressure recovery in terms of spreading angle.

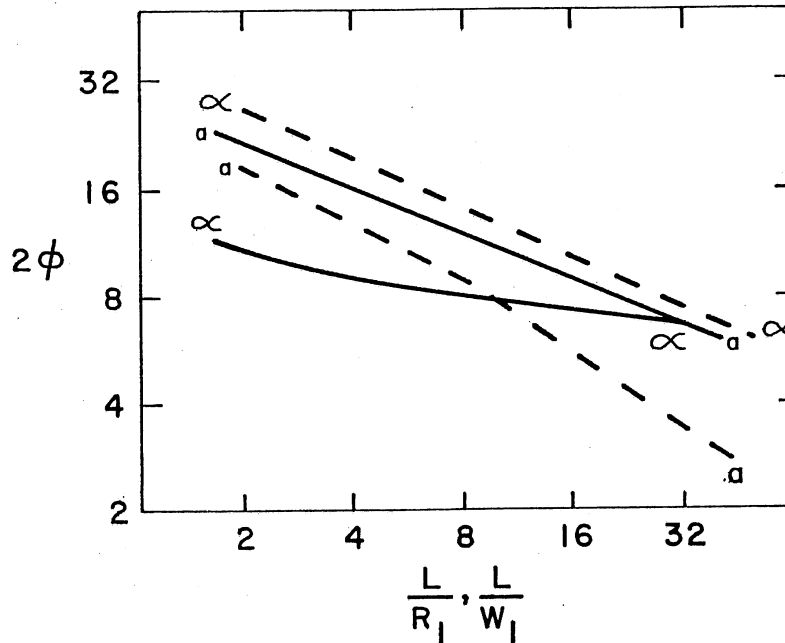


b) Contours of effectiveness in terms of spreading angle.

Fig. 11. Performance data for conical diffusers. (Adapted from McDonald and Fox, 1966.)

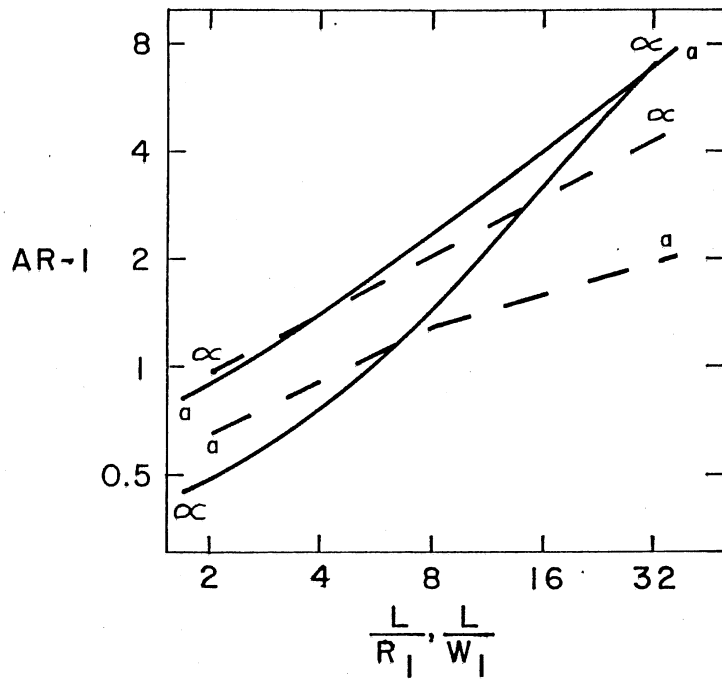


c) Contours of pressure recovery in terms of area ratio.



d) Lines of first appreciable stall (a-a) and of maximum pressure recovery at constant length (α - α).
 — conical diffusers, --- two-dimensional diffusers.

Fig. 11. Performance data for conical diffusers. (Adapted from McDonald and Fox, 1966.)



e) Same as d) but plotted in terms of area ratio.

Fig. 11. Performance data for conical diffusers. (Adapted from McDonald and Fox, 1966.)

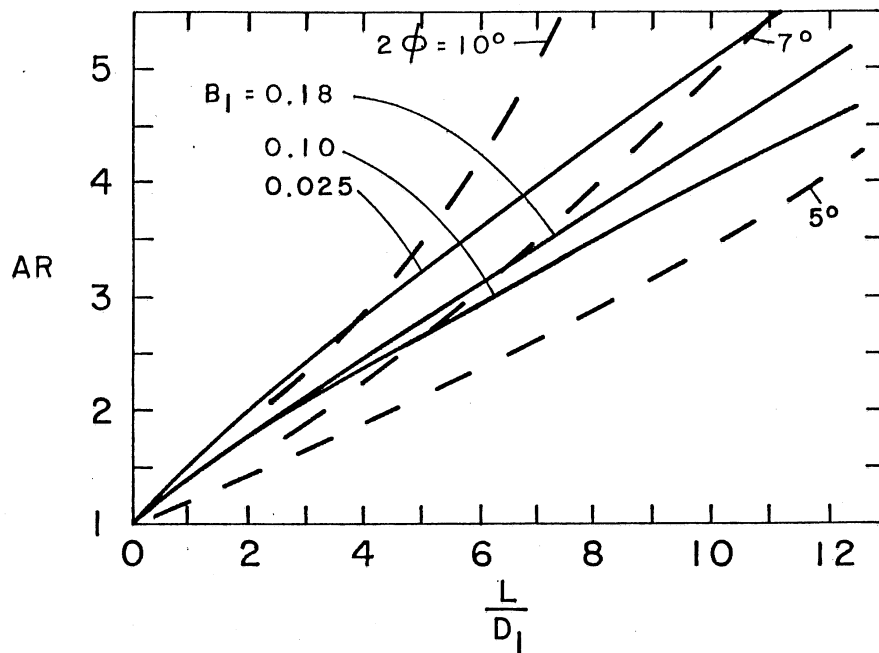


Fig. 12. Optimum diffuser geometries for prescribed dimensionless diffuser length. (Adapted from Klein, 1981.)

It should be noted in passing that a number of investigators present their data obtained with inlet boundary layers of different thicknesses plotted against the ratio of the momentum thickness to the inlet diameter, where for a fully developed turbulent pipe flow $\theta/D \approx 0.05$. It seems to be clear now (Klein, 1981) that a better collapse of data is obtained when using the area blockage ratio B_1 based on the displacement thickness.

Using Fig. 5 of Sovran and Klomp and redrawing it in a different form, we obtain Fig. 13 which shows the maximum achievable pressure coefficient with thin inlet boundary layers and $AR = O(5)$. The broken portion of the curve is a guessed extrapolation of the data, based on the expected decrease of performance at very small cone angles, caused by increasing skin friction losses.

For a fixed diffuser geometry, an increase in blockage brings about a drop in C_p , especially at very low blockages. As blockage increases, C_p levels off and actually increases as B_1 approaches a value of 0.2 appropriate for the fully developed pipe flow, as is seen in Fig. 14 taken from Klein (1981). The surprising increase in C_p at fully developed pipe conditions was discussed by Bradshaw (1963) and Cockrell (1964). The C_p increase seems to be conclusively linked to the higher turbulence level in the entering pipe flow. Using the more appropriate definition $C_p\alpha$, instead of C_p , the pressure coefficient would start at the same value as C_p at $B_1 = 0$, but would be increasingly lower at higher blockages. The upturn in performance at the high blockages would be smaller, or would perhaps disappear.

As we have seen in Fig. 13, increasing the diffuser included angle leads to a rapid deterioration of performance due to flow separation. This trend continues beyond the range shown in Fig. 13, and around 40° the performance is down to that obtained in a plain sudden expansion ($2\phi = 180^\circ$) in pipes of the same area ratio as the diffuser. The energy loss reaches a maximum around $2\phi = 60^\circ$, after which the performance gradually improves as the angle is further increased. The existence of the energy loss maximum at 60° has been shown to exist at least for diffusers followed by tailpipes; it is not certain the same holds for diffusers without tailpipes.

Effects of Turbulence

Enhanced turbulence levels in the inlet flow have been shown to be beneficial to diffuser performance; see Klein (1981), Shárán (1972 and 1976) and Bradshaw (1963). One manifestation of the effects of turbulence is the already mentioned upturn of C_p with increased boundary layer thickness as the fully developed pipe flow condition is approached (Fig. 14). The argument made by Bradshaw concerning this upturn was that it is caused by the larger-size turbulent motions which are better capable to transfer momentum radially than the smaller-scale turbulence of thinner boundary layers; this improves the ability of the boundary layers to remain attached in the adverse pressure gradient. Increasing the thickness of the inlet boundary layers by additional length of pipe ahead of the diffuser, thus produces two opposing effects: an increase in the blockage ratio B_1 , and the change in the turbulence intensity and scale. From Fig. 14 it is apparent that at small boundary layer thicknesses it is the negative effect

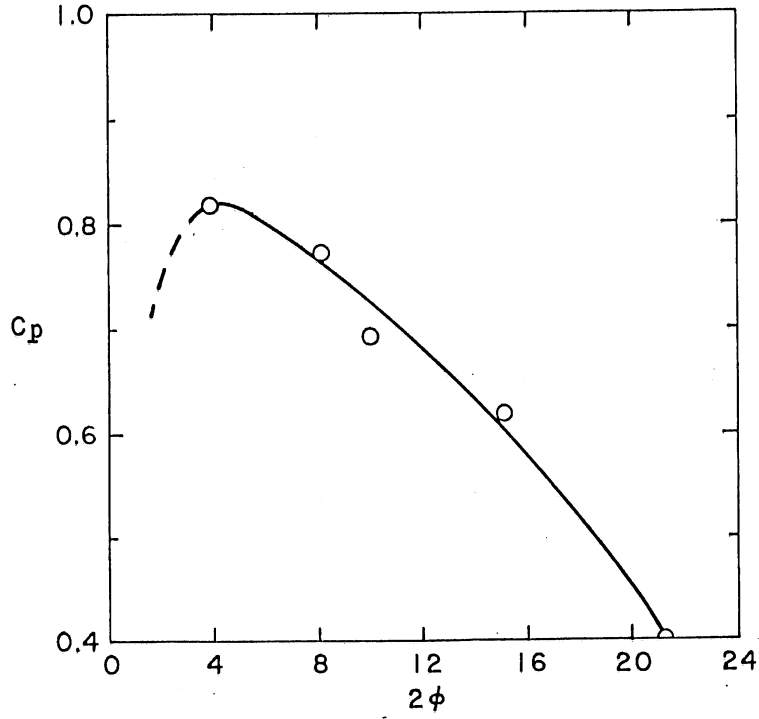


Fig. 13. Maximum pressure recovery at $AR = 5$ and $B_1 = 0.02$.

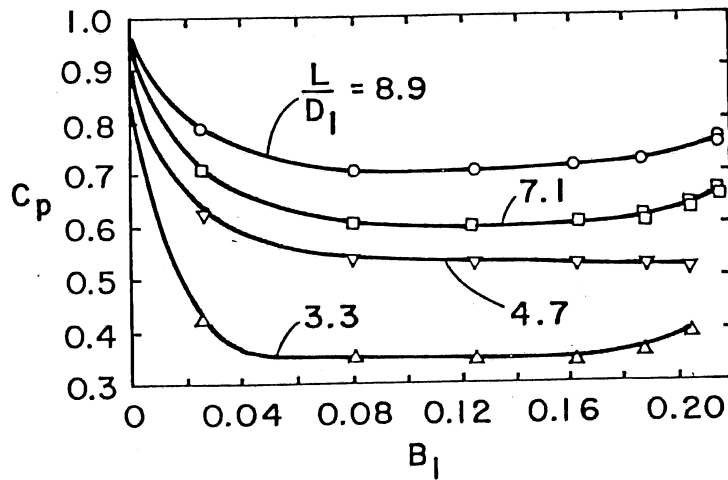


Fig. 14. Effects of inlet blockage on the performance of diffusers with an area ratio $AR = 5$. (Adapted from Klein, 1981.)

of blockage that dominates, while at large thicknesses the beneficial effect of turbulence takes over.

The increased turbulence level not only helps the boundary layers to remain attached, but it also increases the skin friction and the direct energy dissipation within the flow, thus increasing losses. Therefore its overall effect can be beneficial only if the flow would tend to separate in its absence, and the increased mixing keeps the boundary layers attached to a degree which more than offsets the additional losses. This points to its usefulness in wide angle diffusers, where the flow would separate in the absence of enhanced turbulence, and where the skin friction losses and dissipation are reduced due to shorter diffuser length.

Enlarging on these arguments, it may be observed that an inlet profile which has thick boundary layers, but in which turbulence level was artificially suppressed, would tend to give very poor results. By contrast, a uniform inlet profile with a high turbulence level (e.g. generated by a grid) should produce good pressure recoveries. Unfortunately, using a turbulence generating grid to improve the diffuser performance is not a practical concept, as the pressure drop across the grid would certainly more than offset any gains made within the diffuser.

On the other hand, in the present context, it is very encouraging that the flow exiting a turbomachine has a naturally high level of turbulence which should be helpful in obtaining good draft tube pressure recovery with relatively large cone angles.

Distorted Inlet Profiles

The effect of symmetric distortions in the inlet profiles were studied by Waitman et al. (1961), Wolf and Johnston (1969), and Kaiser and McDonald (1980), all of these involving two-dimensional diffusers. The distortions were either of the jet-type, with higher velocity on the centerline and lower near the walls, or of the wake type, with a velocity deficit on the centerline. The jet-type profile starting with low velocity near the walls proved to be prone to early separation and gave results that were substantially worse than for the uniform inlet profile (Wolf and Johnson, 1969).

The wake profiles gave more encouraging results. Depending on the value of the distortion parameter λ , defined by Kaiser and McDonald as

$$\lambda \equiv U_{\max} / U_{\min} \quad (35)$$

where U_{\min} is on the centerline, the wake profile was seen to reduce tendency to separation and to provide in some cases improved performance as well. The wake-type non-uniformity affects the flow in several ways. On the positive side, it increases the flow velocity near the walls and thus it delays flow separation; further, the shear layers in the wake profile generate turbulence which should be beneficial. At the same time, the velocity deficit on the centerline tends to become more pronounced and may become reversed, and this leads to large kinetic energy flux at the exit

and flow unsteadiness. These negative effects become stronger with increasing λ .

The available literature is not very complete. Kaiser and McDonald are the only ones to have studied a range of λ values, going from 1.0 to 2.58. However, they present only lines of first appreciable stall and no pressure rise data (Fig. 15). There is considerable scatter in this data, but it appears that around $\lambda = 1.3$ the centerline velocity deficit provides the maximum benefit, especially at larger diffuser lengths.

Wolf and Johnston (1969) had just one wake profile with $\lambda = 1.73$. This profile appeared to be too non-uniform and showed tendency towards increasing profile non-uniformity, with centerline velocity decreasing in the downstream direction and eventually reaching negative values. The pressure coefficients obtained tended to be lower than for the uniform inlet profile (Fig. 16). The exceptions were short, wide-angle diffusers which had very poor performance with uniform inlet profiles, and were most likely stalled. For these, the data show some improvement, but the pressure recovery achieved is still quite poor.

Waitman et al. (1961) used two wake profiles. One was generated by a splitter plate upstream of the diffuser and was narrow and deep with $\lambda = 1.6$, and the other was generated by a circular rod and was shallow and broad with $\lambda = 1.1$. Comparison of the diffuser performance, between these two profiles and the uniform profile (Fig. 17), as characterized by C_p , shows a substantial improvement for the shallow wake, while the deeper wake gave only a small improvement. Correcting for the effects of increased inlet kinetic energy, i.e. using $C_p\alpha$ to characterize the performance, would reduce the gains, but the shallow wake should still be seen as an improvement.

In summary, the maximum benefit is derived from wake-like inlet profiles. These profiles should be shallow enough to allow diffusion of this non-uniformity within the diffuser; deep wakes tend to grow deeper and eventually degrade the performance. The best results are obtained with $\lambda = 1.1 - 1.3$.

Bent Diffusers

It is very common that a draft tube has to be designed with a curved centerline. Experience shows that curved passages make poor diffusers. Accordingly, a practice has developed whereby elbow draft tubes are designed to diffuse in their straight sections and to have a constant area around the bend. Also, to reduce the radius of curvature on the inner wall, the draft tubes are flattened in the bend area. S-shaped draft tubes cannot do without some diffusing in the bends, as that would mean excessive draft tube length. Fortunately, as will be seen below, the performance of mild bends is affected only weakly by turning through small angles.

The basic diffuser literature has two key papers on the subject, both dealing with 2-D diffusers. Fox and Kline (1962) studied flow regimes (but not performance) of diffusers with circular arc centerlines. Their results, presented in terms of the line of first appreciable stall, are given in

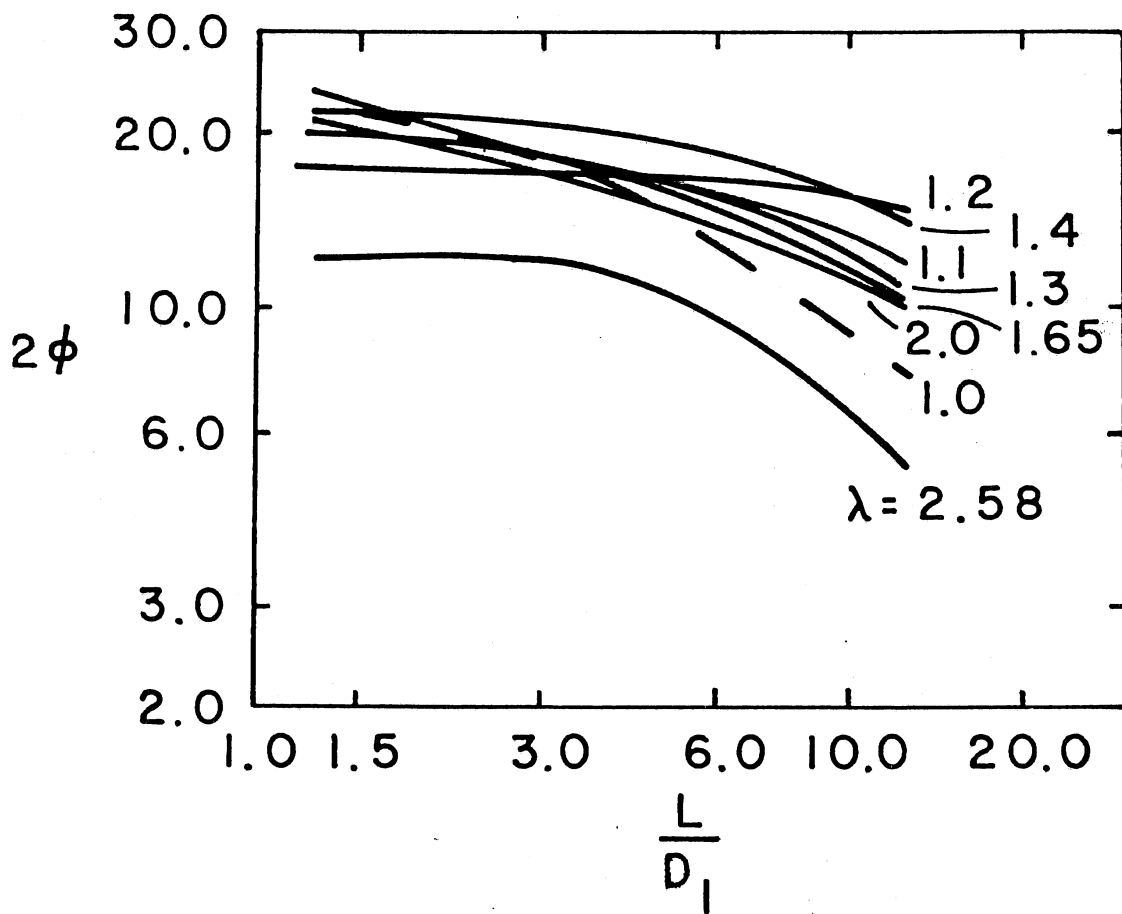


Fig. 15. Lines of first appreciable stall for non-uniform (wake-like) inlet profiles. (Adapted from Kaiser and McDonald, 1980.)

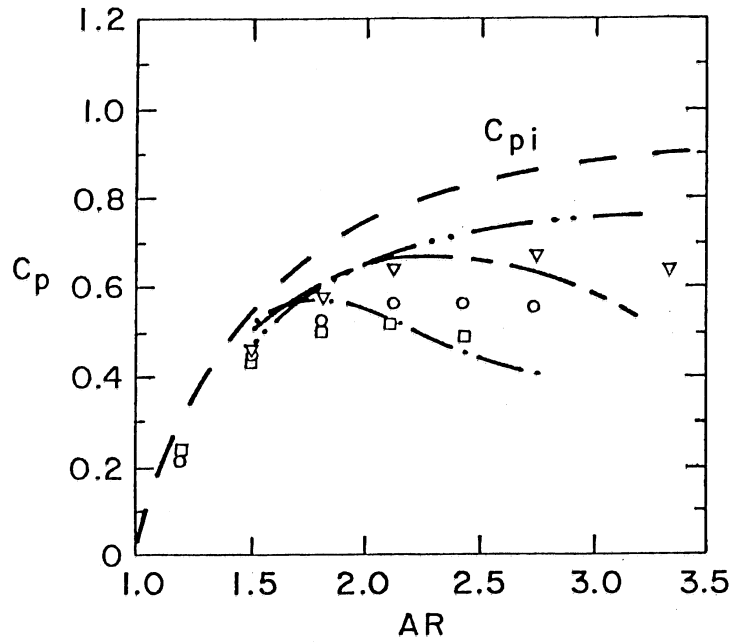


Fig. 16. Comparison of measured pressure recovery of two-dimensional diffusers with wake-like inlet profile (data points) and uniform inlet profiles (lines).
 \square --- $L/W_1 = 3$, \circ --- $L/W_1 = 6$, ∇ --- $L/W_1 = 12$.
 C_{pi} is the ideal, inviscid, pressure coefficient.
 (Adapted from Wolf and Johnston, 1969.)

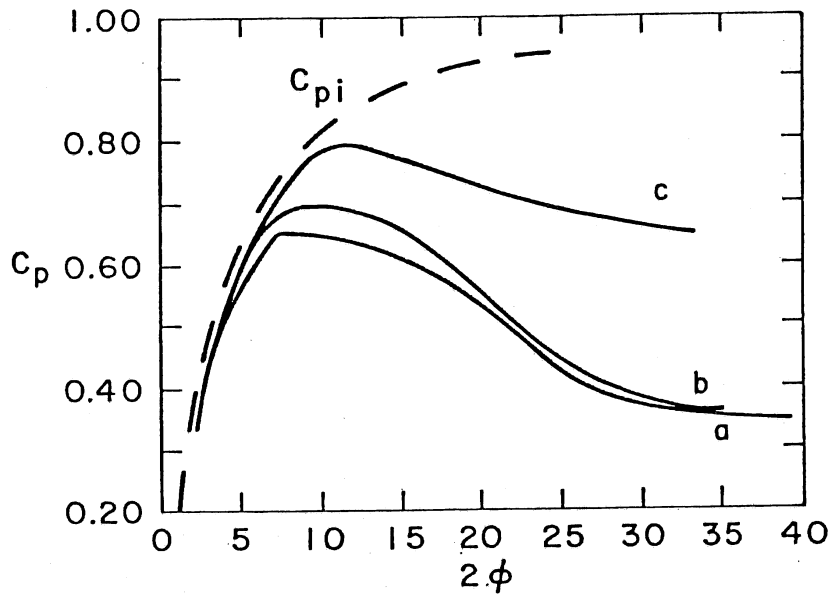


Fig. 17. Comparison of pressure recovery for three different inlet conditions: (a) uniform profile, (b) splitter plate wake profile, (c) rod wake profile. $L/W_1 = 3.0$. (Adapted from Waitman et al., 1961).

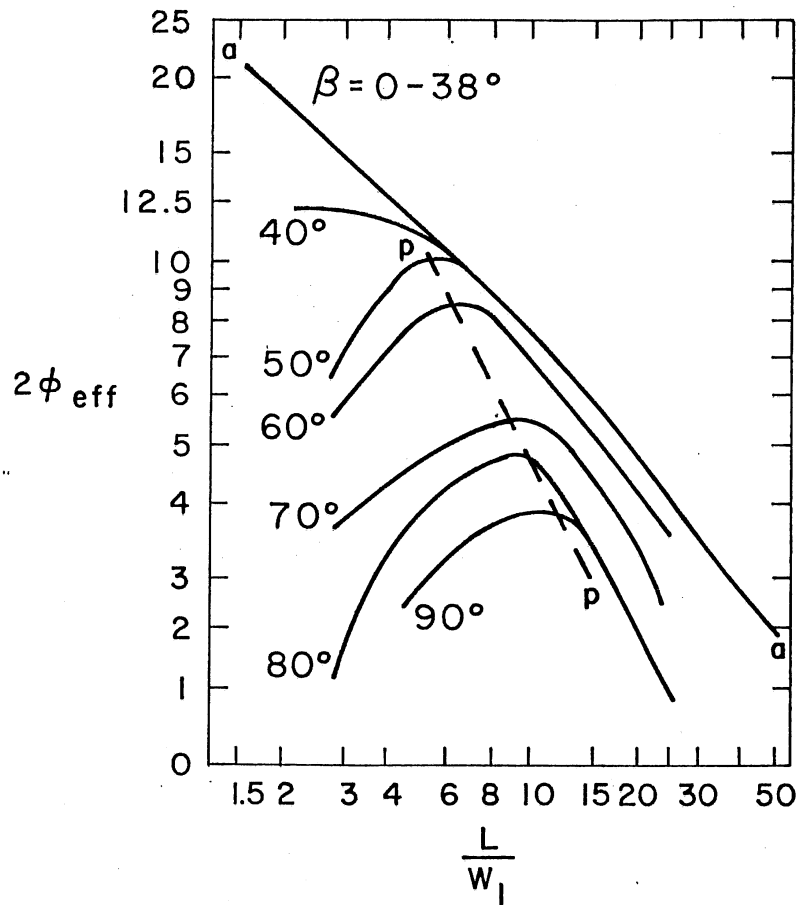


Fig. 18. Location of first appreciable stall (line a-a) as a function of turning angle in curved diffusers with circular arc centerline and linear area distribution. Line p-p denotes maxima of individual curves. (Adapted from Fox and Kline, 1962).

Fig. 18. The figure shows that the onset of the first stall is unaffected by turning up to $\Delta\beta = 30^\circ$. At 40° , a significant drop in the spreading angle appeared at low values of L/W_1 , and beyond 50° the decrease extended over the whole L/W_1 range. Simultaneously, a local maximum developed in the curve, reflecting the excessively small radius of the bend at small values of L/W_1 . It is unfortunate that the paper presented no performance data, but a subsequent paper by Sagi and Johnston (1967) did include a comparison of performance of a number of straight-wall and circular-arc-wall diffusers, all of which were designed at the first-stall limits. The data included the range where the stall limit was the same for both types of diffusers, and it showed that the performance of the circular-arc diffusers was well below the straight-wall ones (Fig. 19).

The investigation of Sagi and Johnston (1967) concentrated on the optimum design of curved diffusers. Their premise was that circular arc is not necessarily the best centerline shape. They observed that the cause of the poorer performance of circular arc diffusers was the unfavorable situation on the inner wall leading to early stall there; the outer wall, on the other hand, was not a problem for the circular-arc designs. They identified three reasons for the difficulty with the inner wall: (1) increase in static-pressure gradients along the inner wall, (2) thickening of the boundary layer due to secondary flows coming from the sidewalls, and (3) suppressed turbulent mixing due to stabilizing flow curvature on the inner wall.

The first point relates to the wall velocity distribution, which instead of a monotonic decrease along the wall, first increases and then rapidly decelerates causing early flow separation. Regarding the second point, they observed that the secondary flows became important only for $\Delta\beta \geq 40^\circ$ which is where the first signs of early stall appear in Fig. 18. And the last point should be accented by noting that the opposite should be happening on the outer wall--enhanced turbulent mixing due to destabilizing curvature should help prevent flow separation there.

Based on these consideration, they reasoned that it should be possible to load the outer wall (which was never observed to stall for $\Delta\beta \geq 30^\circ$) more heavily, taking off some of the load from the inner wall. Accordingly, they developed an analytical inverse design procedure for generation of wall contours for a given wall velocity and pressure distribution, and for given values of AR_1 , L/W_1 and $\Delta\beta$. Examples of the resulting wall shapes are shown in Fig. 20. Subsequent experimental programs showed that their designs were indeed better performers than the circular-arcs of Fox and Kline, although they fell short of equivalent straight-walled diffusers (Fig. 21a-21d).

The experiments also showed that the outer walls could be loaded up to the straight wall stall limits, but not beyond. Apparently, the increase in turbulent mixing on the outer wall was not sufficient to permit a heavier loading. On the inner wall the loadings had to be chosen well below the first stall limit of the equivalent straight wall diffuser in order to prevent stall.

In summary, it appears that one can safely diffuse the flow through turns up to $\Delta\beta = 30^\circ$. Beyond this bend angle the performance gets

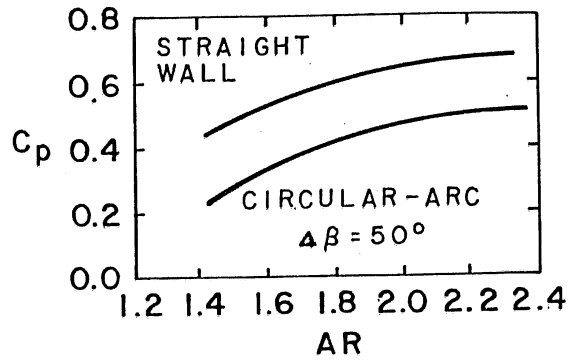


Fig. 19. Performance of circular-arc designs of curved diffusers at first-stall limits for $\Delta\beta = 50^\circ$, contrasted to performance of straight wall diffusers at their first-stall limits. (Adapted from Sagi and Johnston, 1967.)

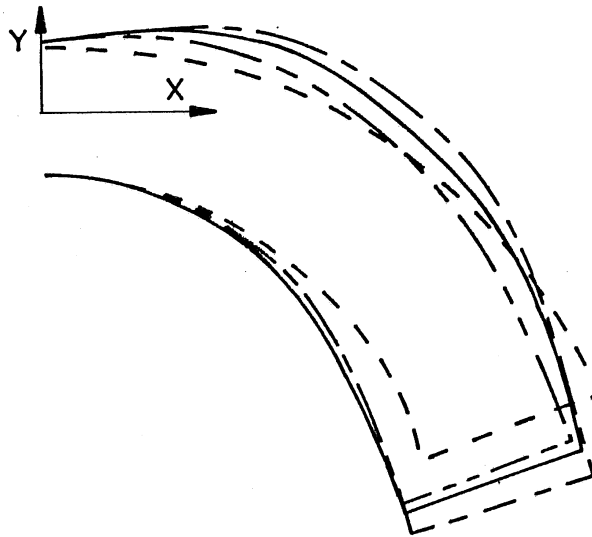
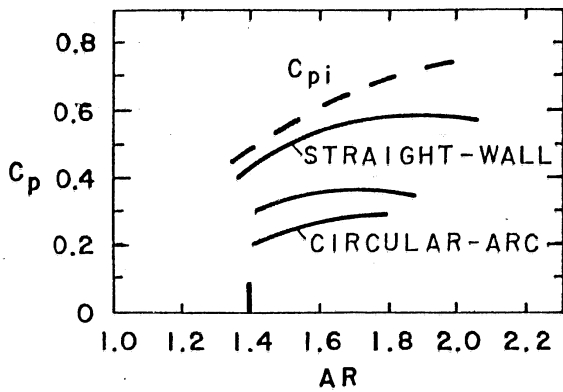
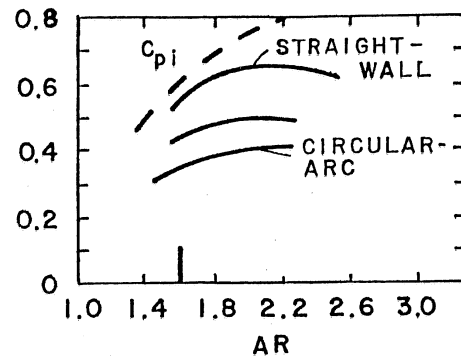


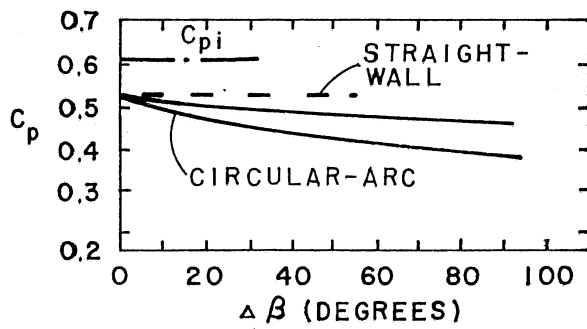
Fig. 20. Comparison of typical curved diffuser shapes for $\Delta\beta = 70^\circ$, obtained by an inverse design procedure, to circular-arc shape (denoted by ---). (Adapted from Sagi and Johnston, 1967).



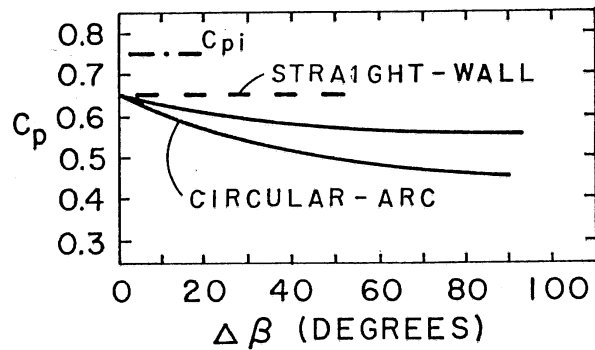
a) $L/W_1 = 4, \Delta\beta = 70^\circ$



b) $L/W_1 = 6, \Delta\beta = 70^\circ$



c) $L/W_1 = 10, AR = 1.6$



d) $L/W_1 = 10, AR = 2.0$

Fig. 21. Performance comparison of straight wall, circular-arc and inverse-design shape diffusers. In all cases the inverse designs lie in between the straight wall and the circular arc diffusers. (Adapted from Sagi and Johnston, 1967.)

increasingly worse. If larger turns must be made in diffusing passages, one should follow the strategy of Sagi and Johnston in developing their shape.

B. Effects of Swirl on Diffuser Flow

Definition of Swirl Ratio

In order to be able to correlate data on the effect of swirl, one has to define some dimensionless parameter representing the swirl magnitude. The local swirl angle (formed by the tangential and the axial velocity components) varies with radius; therefore, it is not easy to pick a value which would be representative.

It is clear that any global value will be imperfect because the swirl velocity profiles may have different shapes, but some choice has to be made to allow analysis of data from different experiments. One possible choice, favored in one form or another by a number of investigators, is a swirl ratio defined as the ratio of the overall angular momentum to the axial momentum. For the diffuser throat one can write

$$M = \frac{\int \rho V_{\theta} V_z r dA}{L \int \rho V_z^2 dA} \quad (36)$$

where L is some characteristic length, reasonably defined as $L \equiv 1/A \int r dA = 2/3R$.

For solid body rotation and uniform axial velocity, it may be shown that

$$M = 3V_{\theta w}/4V_z \quad (37)$$

where $V_{\theta w}$ is the tangential velocity near the wall outside of the boundary layer. For the Rankine vortex one obtains

$$M = 1.5 V_{\theta w}/V_z \left[1 - \frac{1}{2} \left(\frac{R_o}{R} \right)^2 \right] \quad (38)$$

where R_o is the core radius of the Rankine vortex profile. Defining now the swirl angle as

$$\tan \delta \equiv \frac{\int V_{\theta} dA}{\int V_z dA} \quad (39)$$

we obtain for a solid body rotation and a uniform axial flow

$$\tan \delta = \frac{2}{3} \frac{V_{\theta w}}{V_z} = 8M/9 \quad (40)$$

and for a Rankine vortex

$$\begin{aligned} \tan \delta &= 2 \frac{V_{\theta w}}{V_z} \left(1 - \frac{2}{3} \frac{R_o}{R} \right) \\ &= \frac{4}{3} M \left(1 - \frac{2}{3} \frac{R_o}{R} \right) / \left(1 - \frac{1}{2} \left(\frac{R_o}{R} \right)^2 \right) \end{aligned} \quad (41)$$

which translates into $4M/3$, $1.1 M$, $0.95 M$ and $8M/9$ for $R_o/R = 0, 0.333, 0.666$ and 1 , respectively. Since any real distribution will be somewhere between the solid body and the Rankine profiles, one can write, in general,

$$\tan \delta \approx M \quad (42a)$$

and in particular,

$$\tan \delta = \frac{2}{3} \frac{V_{\theta w}}{V_z} \quad (\text{solid body}) \quad (42b)$$

$$\tan \delta = \frac{2V_{\theta w}}{V_z} \left(1 - \frac{2}{3} \frac{R_o}{R} \right) \quad (\text{Rankine}) \quad (42c)$$

These are the definitions that we shall use. In the following paragraphs we shall review the definitions found in the literature and relate these to the present definitions.

Cassidy (1969) proposed a definition for a dimensionless parameter in the form

$$m_1 = \frac{\Omega D}{\rho Q} \quad (43)$$

where Ω is the theoretical angular momentum entering the draft tube and Q is the volumetric rate. Since M , defined above, may be written as

$$M = \frac{\Omega}{\rho Q V_z} \frac{2}{3} R = \frac{\Omega D}{\rho Q} \frac{3\pi}{4} \quad (44)$$

it follows that

$$m_1 = \frac{4}{3\pi} M \quad (45)$$

Other investigators, e.g. Shaalan and Shabaka (1975) and Neve and Thakker (1981) used as the definition of the swirl angle the setting angle of radial vanes at the inlet to the diffuser (Fig. 22). Assuming that the flow follows the vanes (just as Cassidy assumes in his definition), then it may be shown that

$$\tan \beta = \frac{\Omega}{\rho Q} \frac{2\pi B}{2} = M \frac{8B}{3D} \quad (46)$$

Assuming that a perfect free vortex is formed following the turn, and substituting accordingly for M , one obtains the relation between the vane setting angle and the effective swirl angle.

$$\tan \delta = \frac{D}{2B} \tan \beta \quad (47)$$

Senoo et al. (1978) use a definition of a swirl parameter

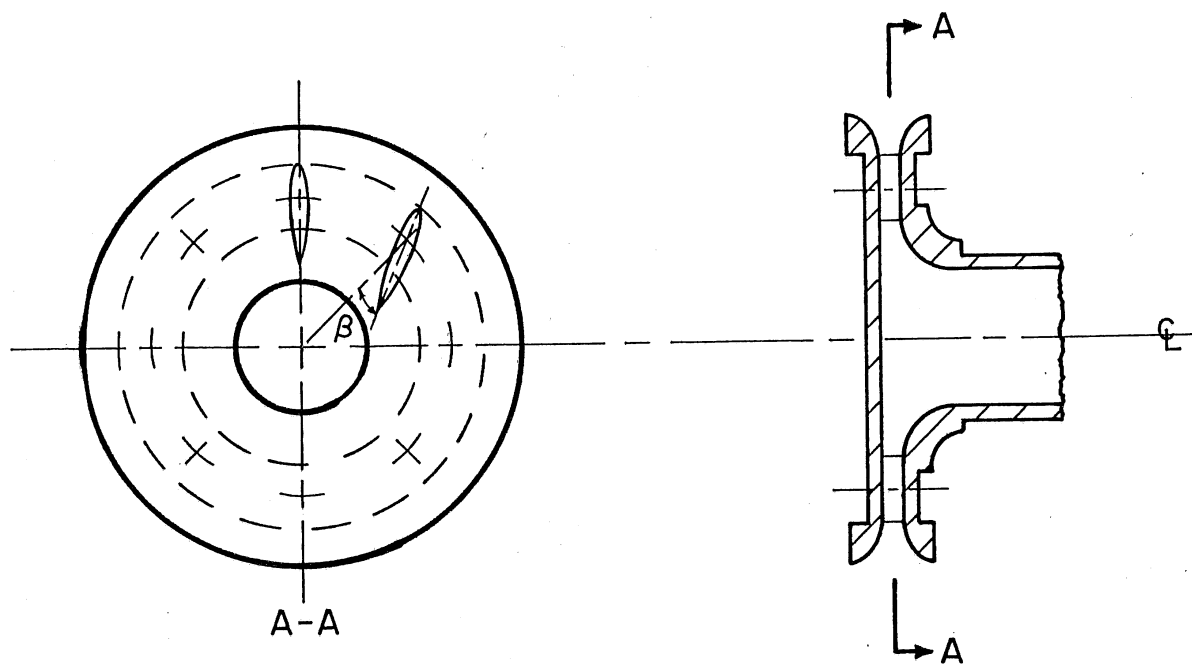


Fig. 22. Typical design of a swirling flow generator producing Rankine vortex-type distribution. (Adapted from Neve and Thakker, 1981).

$$m_2 \equiv \frac{\int V_z V_\theta r^2 dr}{R \int V_z^2 r dr} \equiv \frac{2}{3} M \quad (48)$$

and they actually perform the indicated integration of the velocity profiles at the diffuser throat to calculate M . For a perfect free vortex one then finds, $\tan \delta = 2m_2$.

Effects of Weak and Medium Swirl ($\delta < 30^\circ$)

Superposition of swirl on the axial flow causes the axial velocity to redistribute itself, decreasing at the centerline and increasing near the walls. This tends to increase the kinetic energy of the flow in two ways: one is the direct addition of the kinetic energy of the tangential motion, and the other is the effect of increased factor α at the inlet. The excess axial velocity at the wall and the additional turbulence production near the wall due to the swirl component have positive influence on the boundary layer flow, helping it to remain attached, and so higher pressure recovery may be achieved. To be useful, this increase in pressure recovery has to be large enough to more than offset the increase in the inlet kinetic energy.

A suitable performance parameter describing the pressure rise is a pressure coefficient defined as

$$C_{p_{\alpha\beta}} = \frac{\bar{p}_2 - \bar{p}_1}{(\alpha_1 + \beta_1) \bar{q}_1} \quad (49)$$

where

$$\bar{p} \equiv \int p v_a dA/Q \quad (50)$$

In the absence of swirl and at moderate cone angles, the pressure is reasonably uniform across the diffuser diameter, and it may be pulled out of the integrals. When swirl is present, there is always some pressure differential between the wall and the centerline (higher on the wall). For solid-body rotation this differential is

$$\Delta p = \int \rho \frac{V_\theta^2}{r} dr = \frac{1}{2} \rho V_{\theta w}^2 \quad (51)$$

or in a dimensionless form

$$\frac{\Delta p}{\frac{1}{2} \rho V_z^2} = \frac{\Delta p}{q_1} = \left(\frac{V_{\theta w}}{V_z} \right)^2 \quad (52)$$

For a Rankine vortex

$$\Delta p = \frac{1}{2} \rho V_{\theta w}^2 \left[2 \left(\frac{R}{R_o} \right)^2 - 1 \right] \quad (53)$$

where R_o is the radius of the inner solid-body core; in a non-dimensional form we have

$$\frac{\Delta p}{q_1} = \left(\frac{V_{\theta w}}{V_z} \right)^2 \left[2 \left(\frac{R}{R_o} \right)^2 - 1 \right] \quad (54)$$

For small swirl angles this pressure differential is not too large: for $\delta = 5^\circ$ and solid body rotation $\Delta p/q_1 = 0.017$, and for Rankine vortex with $R_o/R = 0.333$, $\Delta p/q_1 = 0.054$. The difference between the wall pressure and the volume averaged pressure is about half that much. At higher swirl angles, however, taking the wall state pressure instead of the average would give excessive errors. In such cases one can get around the problem by using Eq. (52) and (54) to deduce the required corrections for the wall pressure.

Five papers dealing with the effect of swirl on performance of conical diffusers were found in the literature: McDonald et al. (1971), Acrivlellis (1977), Senoo et al. (1978), Neve and Wirasinghe (1978), and Neve and Thakker (1981).

McDonald et al. (1971) studied the effects of swirl on 24 diffusers with included angles $2\phi = 4, 6, 8, 12, 15.8$ and 31.2° and area ratios of 1.3, 1.6, 2.4, 4.5, and 8.3. The Reynolds number at the inlet plane was 150,000. A solid-body swirl of three different magnitudes was produced by a rotating honeycomb. The paper gave the tangential velocity profiles, but not the axial ones. Calculating the average axial velocity from the Reynolds number, one finds

$$\delta = \tan^{-1} 2/3 V_{\theta w}/V_z = 7.6^\circ, 10.2^\circ \text{ and } 18.4^\circ$$

The results are presented in terms of a pressure coefficient

$$C_{PRS} \equiv \frac{(1/A \int p dA)_2 - (1/A \int p dA)_1}{\rho/2(1/A \int V^2 dA)_1} \quad (55)$$

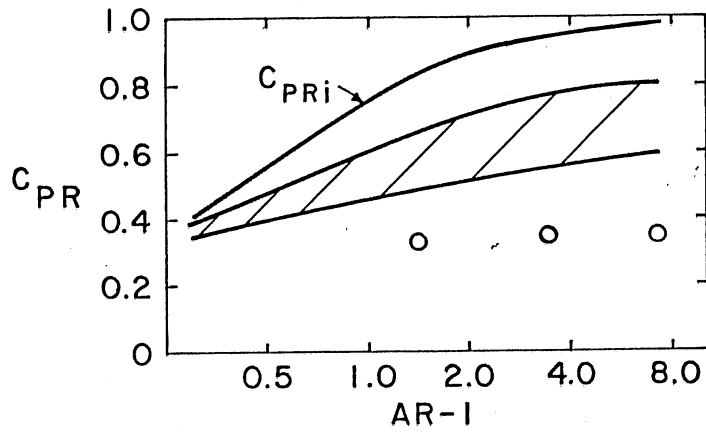
where V is the magnitude of the total velocity vector including the swirl. This coefficient is almost the same as $C_{p_{\alpha\beta}}$ except for the manner in which one calculates the pressure average over the inlet and exit planes. The results are shown in Figs. 23a and 23b comparing the cases of the strongest swirl ($\delta = 18.4^\circ$) and of no swirl. The swirl is seen to improve the performance at all divergence angles, except for $2\phi = 31.2^\circ$ where the flow apparently remained separated even with the swirl present. The strong improvement found at small cone angles is contrary to data of others which will be discussed below. Also, the high recoveries with C_{PRS} approaching unity seem unrealistic. It is felt at this time, that either the data or their presentation are not reliable.

The paper of Acrivlellis (1977) deals with diffusers with total included angles of 8, 10, 12, 14, and 16° . There was also some variation in the diffuser length and area ratio, but no clear details were given. Reynolds number at the inlet was set at 128,000. Rankine vortex swirl was produced by circumferential adjustable vanes set at 0, 10, 20, 30, 40, and 50° , through which the flow entered radially and then turned in the axial direction into the diffuser (Fig. 22). Unfortunately, the definition of several key parameters and coefficients are missing in the paper, being replaced by references to another paper by Schiebeler (1955). That paper could not be obtained and without it not much can be gleaned from Acrivlellis' paper.

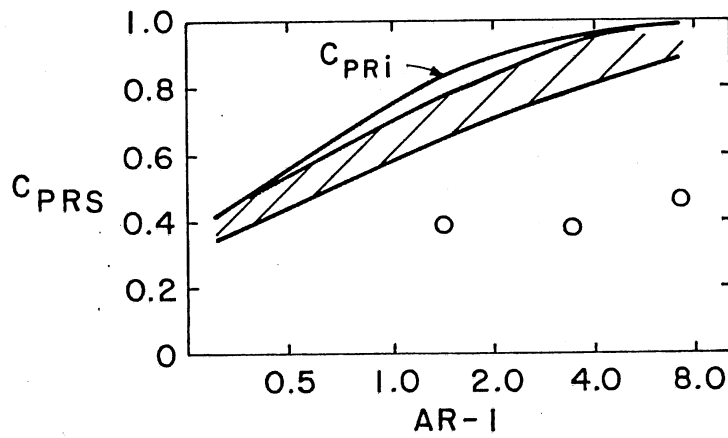
Senoo et al. (1978) studied conical diffusers with total angles of 8, 12, 16, 20 and 30° , all with area ratio of four. The axial velocity was not given, but the inlet diameter was 153 mm, so the Reynolds number is likely to have been over 100,000. The swirl was again produced by circumferential vanes, and its magnitude was characterized by a parameter m_2 discussed earlier, obtained by actual integration of the velocity profiles. Three different swirl levels were produced

$$\delta = \tan^{-1} 2m_2 = 8^\circ, 13.5^\circ, 19.8^\circ$$

The profiles of the tangential velocity component were almost perfect Rankine vortices. These classical Rankine profiles persisted through the diffusers despite noticeable broadening of the inner core. The axial velocity profiles at the inlet plane all had a strong dip in the center, presumably caused by the swirl, but otherwise were uniform. At the diffuser outlet the profiles were peaked near the wall, as opposed to the no-swirl case where the profile was peaked at the center. The α factor of the exit profiles was much smaller with swirl than without. The results were presented in terms of three different pressure coefficients. Of these, C_{pr} appears to be equivalent to $C_{p_{\alpha\beta}}$; therefore, it was chosen to be plotted in Fig. 24. It is seen that the optimum swirl angle increases with



a) Axial inlet flow.



b) Swirling inlet flow, highest swirl $\delta = 18.4^\circ$.

Fig. 23. Diffuser performance coefficient as a function of area ratio. Shaded area covers cone spreading angles in the range $2\phi = 4^\circ - 15.8^\circ$, symbols show results for $2\phi = 31.2^\circ$. (Adapted from McDonald et al., 1971.)

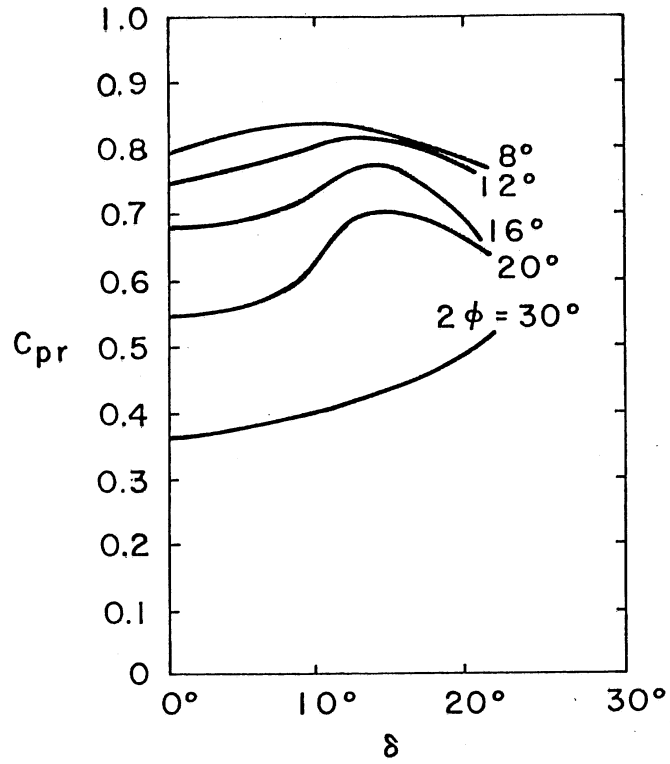


Fig. 24. Pressure recovery coefficients as a function of swirl angle at $AR = 4$. (Adapted from Senoo et al, 1978.)

increasing cone angle, a fact noted by a number of investigators. What is important is that at all cone angles there was a range of swirl angles for which the overall performance was better with swirl than without it. The gain was fairly small for the small-angle diffuser with $2\phi = 8^\circ$. The improvement was quite impressive for the 20° cone, although the pressure rise still remained well below that of the 8° cone.

Neve and Wirasinghe (1978) investigated three diffusers with total angles of 10° , 20° and 30° , all of them with area ratio of four, followed by a constant area tailpipe. The Reynolds number was on the order of 50,000. Solid body rotation was generated by a spinning honeycomb. Three swirl ratios were generated, for which the paper quotes swirl angles of 6.8° , 10.9° , 15° , respectively, but unfortunately they do not say how the swirl angle is defined. (Using their Fig. 4 and the given value of the Reynolds number, one obtains $\alpha = \tan^{-1} \frac{2}{3} V_{\theta w} / V_z = 8.8^\circ$ for the middle swirl. Using this as a guide, it appears that their definition of swirl angle gives values which are about 20 percent higher than those given by the present definition of the swirl angle.) The results are presented in terms of two pressure coefficients, one of which is the classical pressure coefficient $C_p \equiv \Delta p / q_1$, where the pressure at the diffuser throat was not corrected for radial pressure gradient (Fig. 25a). An attempt was made to calculate $C_{p\alpha\beta}$ from the presented C_p . Values of α_1 were available for two of the swirl levels (Fig. 25b), but had to be estimated for the lowest swirl. Values of β_1 could be calculated, yielding 0.009, 0.014 and 0.027 for $\alpha = 7^\circ$, 8.8° , and 12.2° , respectively. The results are displayed in Fig. 26. The swirl is seen to degrade the performance of the 10° diffuser, but provides increasing benefits with increasing spreading angle. Simultaneously, the peak in $C_{p\alpha\beta}$ shifts toward higher swirl levels as cone angle increases.

Neve and Thakker (1981) studied the same three diffusers as the previous paper, i.e. total angles of 10° , 20° , and 30° followed by a tailpipe. The Reynolds number was about 40,000. The main difference from the earlier study was that the swirl was generated by circumferential vanes set at angles between 4 and 20° to produce Rankine vortex distributions of different strengths. The initial swirl profiles were Rankine type, but they tended rapidly towards solid-body shapes within the diffuser (unlike the profiles observed by Senoo et al). Using sketches given in the paper as a guide, one could calculate the swirl angle from the vane setting angle as

$$\tan \alpha = \frac{D}{2B} \tan \beta = 3.55 \tan \beta$$

which means that the produced swirl angles were very high, up to 50° . The paper gives swirl and axial profiles for case $\beta = 10^\circ$ and this information was used to check the above equation; a very good agreement was found. The results were presented in terms of C_p and also in terms of a loss coefficient. Based on their data expressed as a ratio of the pressure coefficients for the swirling case to the non-swirling case (Fig. 27), the authors concluded that there is not much improvement for cones whose total angle is less than about 8° because in such cases increased friction offsets any advantages due to swirl. Best result was found for cone angle of 20° with vane angle of 10° , equivalent to 32° swirl angle. However, since

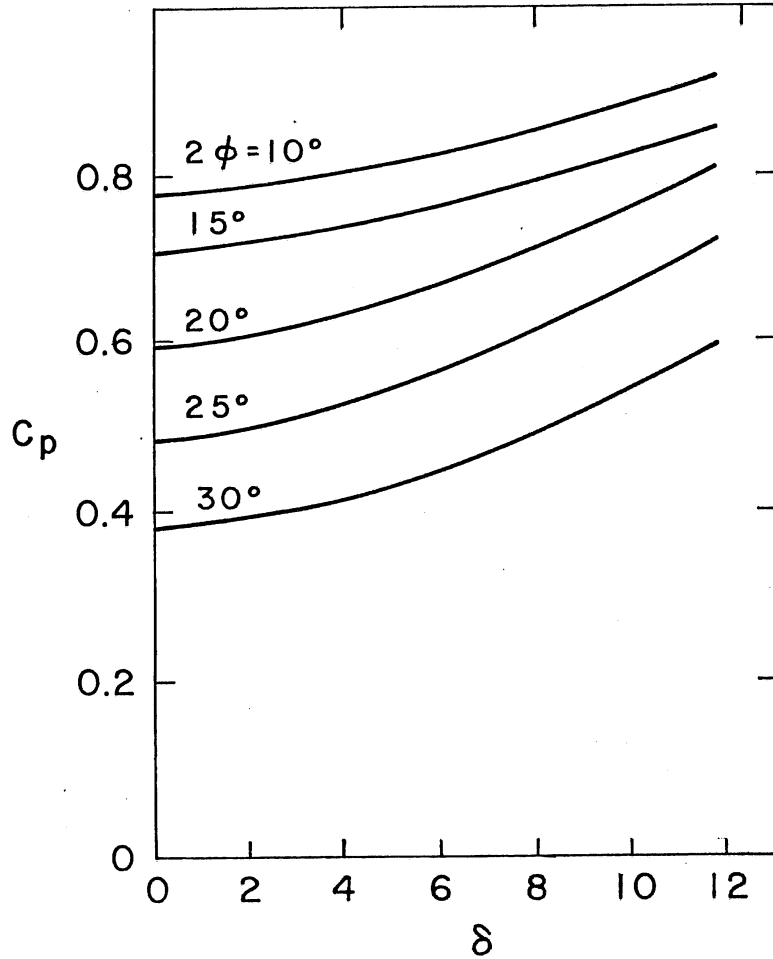


Fig. 25a. Effect of swirl on static pressure coefficient C_p at $AR = 4$. Diffuser is followed by a tailpipe. (Adapted from Neve and Wirasinghe, 1978.)

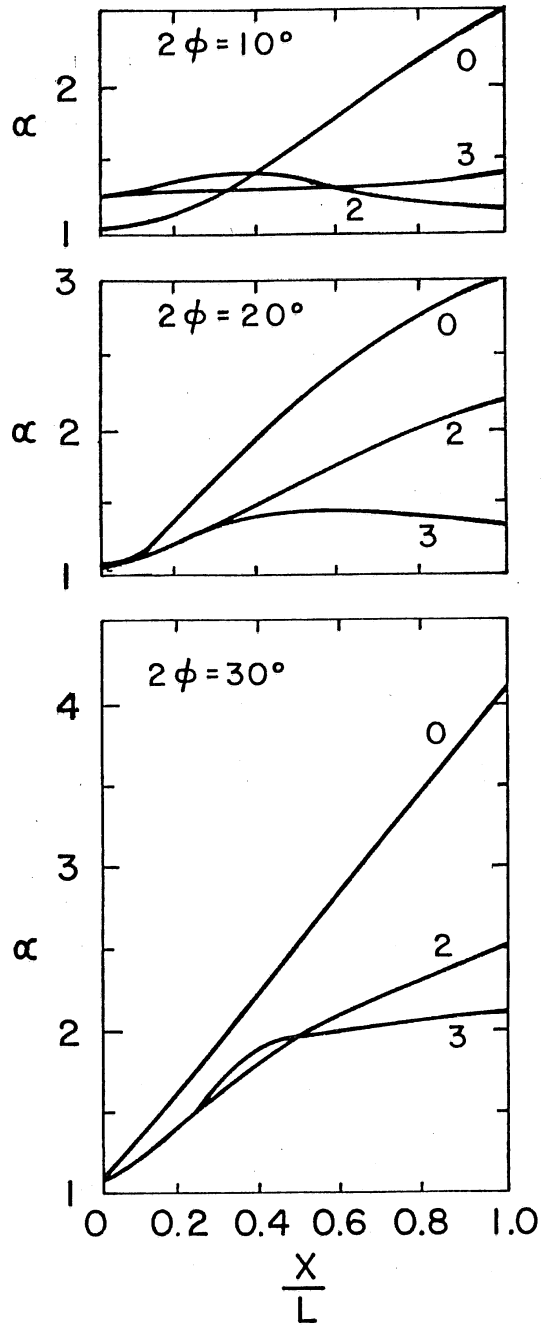


Fig. 25b. Effect of swirl on kinetic energy factor α along the diffuser length. (Adapted from Neve and Wirasinghe, 1978.)

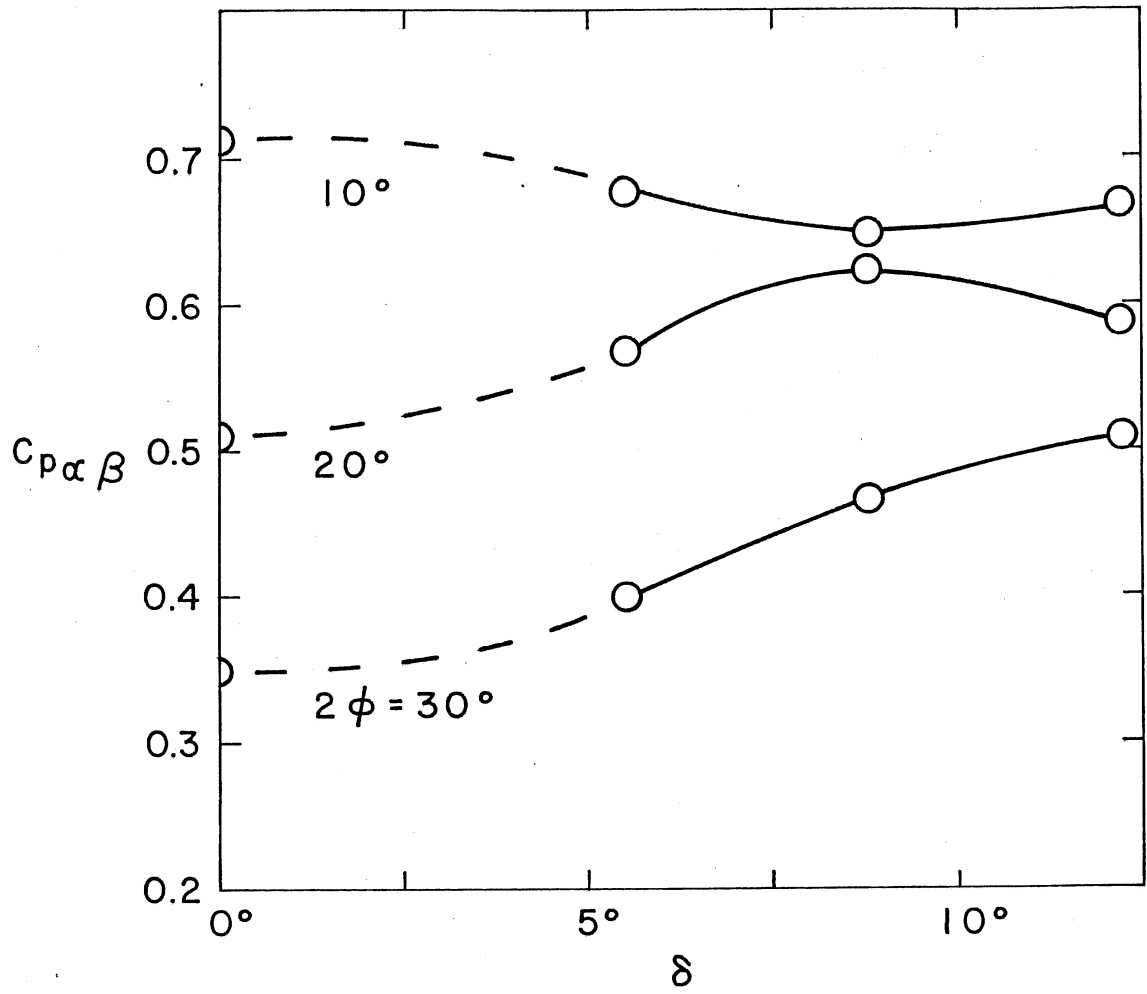


Fig. 26. Pressure coefficient $C_{p\alpha\beta}$ extracted from data in Figs. 24 and 25.

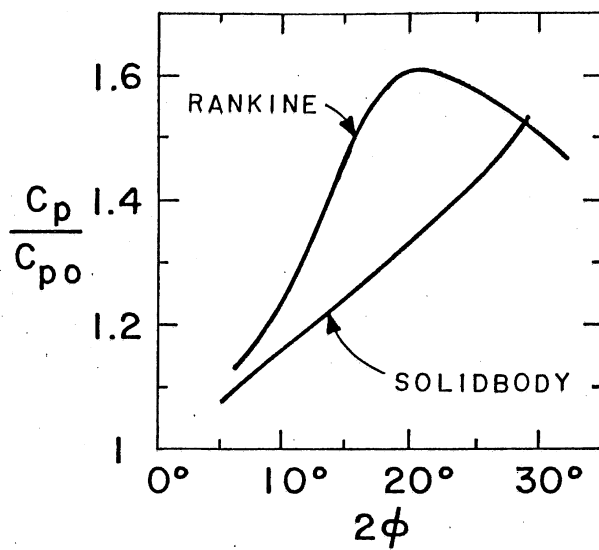


Fig. 27. Ratio of pressure coefficient for swirling case to pressure coefficient for non-swirling case for AR=4. (Adapted from Neve and Thakker, 1981.)

the definition of C_p neglects the inlet kinetic energy due to swirl, the improvements must be corrected downwards, especially so in view of the large swirl angles used. They also noted that the Rankine vortex distribution gave better results at small cone angles, while the solid body rotation tended to be better at higher cone angles. (The Rankine vortex flow had much higher swirl angle, however).

Effect of Strong Swirl

As the swirl is increased further, a flow reversal appears on the centerline. It has been reported by So (1967) to appear first at the inlet plane of the diffuser from where it was extending downstream with increasing swirl (total angle 10° - 70°), but Cassidy (1969) and Harvey (1962) report the onset at the exit of a constant area tube from where it was extending upstream with increasing swirl. The difference in these findings may be due to the fact that one was established in the diffuser, while the other two were observed in a constant area duct.

Harvey's data indicated that the vortex breakdown (onset of velocity reversal) occurred in his low-speed, laminar, flow at a swirl angle of 51° , in agreement with the theory of Squire (1960). In the experiments of Cassidy the onset of the reversed flow occurred at angular momentum parameter values of 0.15-0.25, depending on the tube length to diameter ratio (Fig. 28). This corresponds to a swirl angle $\alpha = \tan^{-1}(3\pi/4)(4/3)(0.15 \div 0.25) = 25^\circ \div 38^\circ$. There is a lack of clarity in the literature coming from the U.S. Bureau of Reclamation on whether the onset of the reverse flow means an onset in flow surging. Cassidy (1969) presents two curves of critical swirl rates (Fig. 28), one pertaining to onset of flow reversal at the tube exit, the other to fully developed surge (at 60-100 percent larger swirl rates). However, elsewhere in the paper he says that at higher speeds surging appeared simultaneously. It seems that the two events do not coincide in laminar flow, but they do at high Reynolds numbers; it should be pointed out, however, that Cassidy (1969) and Cassidy and Falvey (1970) do not state this explicitly. A later publication by Falvey (1971) shows sketches of flow regimes in diffusers, which indicate that the onset of surging in turbulent flow coincides with the onset of the reverse flow (Fig. 29).

According to the extensive data of Palde (1972), taken at the U.S. Bureau of Reclamation,² the onset of surging in model draft tubes tended to fall above $m_a = \Omega D / g Q^2 = 0.4$ or

$$M > 0.94 \quad (56)$$

which corresponds to $\alpha = \tan^{-1} 4/3 M = 51^\circ$, a number which is in agreement (most likely by coincidence) with the values mentioned earlier as corresponding to vortex breakdown. The data was taken in an air flow facility, and the inlet diameter of the draft tubes was about 6 inches. The Reynolds number of the experiment was not given, but it was likely to have been more than 10^5 ; therefore the flow was turbulent.

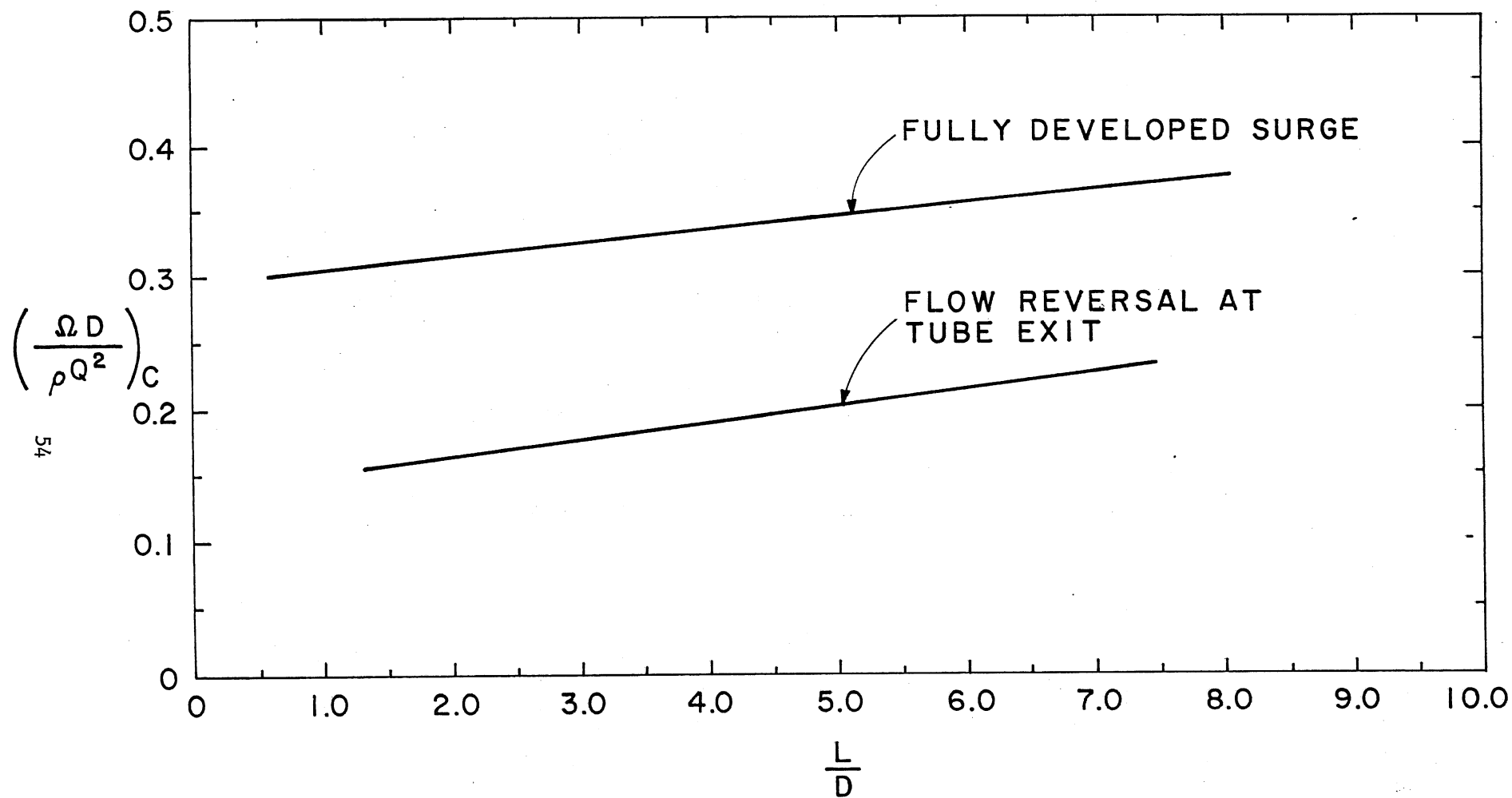


Fig. 28. Lines of critical swirl rates for onset of flow reversal at tube exit and for fully developed surge. (Adapted from Cassidy, 1969.)

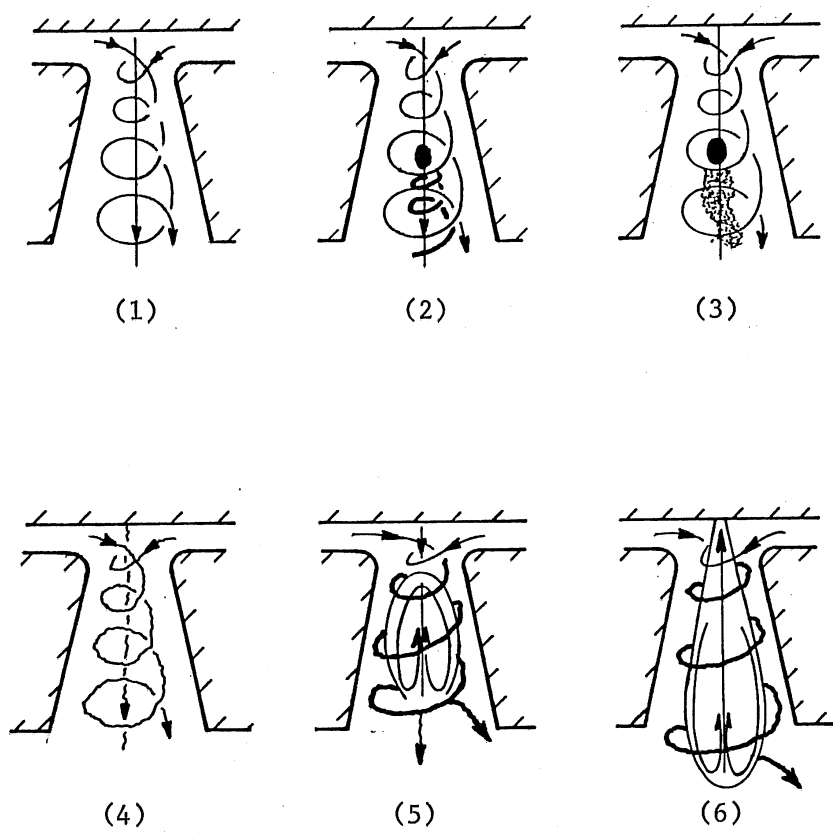


Fig. 29. Flow regimes with swirling flow in divergent conduits. (Adapted from Falvey, 1971).

- Regime 1 - Weak swirling flow, laminar throughout. No surging.
- Regime 2 - A disturbance forms on axis. Flow laminar throughout. Surges.
- Regime 3 - Laminar flow upstream from disturbance, turbulent downstream. No surging.
- Regime 4 - Turbulent throughout. No surging.
- Regime 5 - Stall on centerline of conduit. Turbulent throughout. Surge irregular.
- Regime 6 - Stall extends throughout conduit. Flow entirely turbulent. Surge is regular when stall region is small, irregular when stall region is large.

The phenomenon of surging was attributed by Cassidy (1969) and his co-workers to the precessing motion of the helical vortex which sets itself up around the reverse flow region on the centerline, shown schematically in Fig. 29. This is plausible, judging from the dimensionless frequency

$$f \frac{D^3}{Q} = 0.85 - 1.5 \quad (57)$$

which is too high to be attributable to "breathing" or washout of the recirculating region, and seems about right for disturbance in the radial direction (Fig. 30).

As for the amplitude of surging, it increases monotonically in constant area cylindrical tubes up to very large values of the swirl parameter, but for diffusing passages the amplitude reaches a maximum around $\Omega D/gQ^2 = 1.2 - 1.3$ (Fig. 31) after which it decreases fairly rapidly. The diffusing passages also have lower surging frequencies, most likely due to the increase in the diffuser diameter with which the surge scales (Fig. 32). A later work by Palde (1972) on the effects of diffuser cone angle suggests that the surge might be reduced by using a diffuser cone angle of 15° , and perhaps eliminated entirely with greater angles. (Palde found no surge in 30° diffusers.)

Summary of Swirl Effects

- (1) Swirl ratio M and swirl angle were defined and are given by expressions (36), (39), and (42).
- (2) Performance coefficient $C_{p\alpha\beta}$ relevant to swirling flows was defined and is given by Eq. (49).
- (3) Five papers dealing with weak and medium swirls were reviewed. Of these, three had Rankine vortex inlet profiles and two had solid body rotation.
- (4) These papers show that moderate swirl can significantly improve the performance of diffusers with cone angles larger than 10° .
- (5) There is some disagreement on the effects of swirl at cone angles smaller than 10° . Some data indicate small but positive improvement, while others show degradation of performance. It seems though, that at cone angles on the order of $5-8^\circ$ and uniform inflow the diffusers are near optimum, and that they have little to gain from addition of swirl.
- (6) At larger cone angles where the flow tends to separate in the non-swirling case, swirl addition can provide impressive gains in pressure rise. Up to $2\phi = 20^\circ$ swirl addition can restore the pressure rise to levels not too much lower than the small angle diffusers. However, the performance starts dropping sharply at angles larger than 20° .
- (7) The swirl level needed for optimum performance increases with the cone angle.

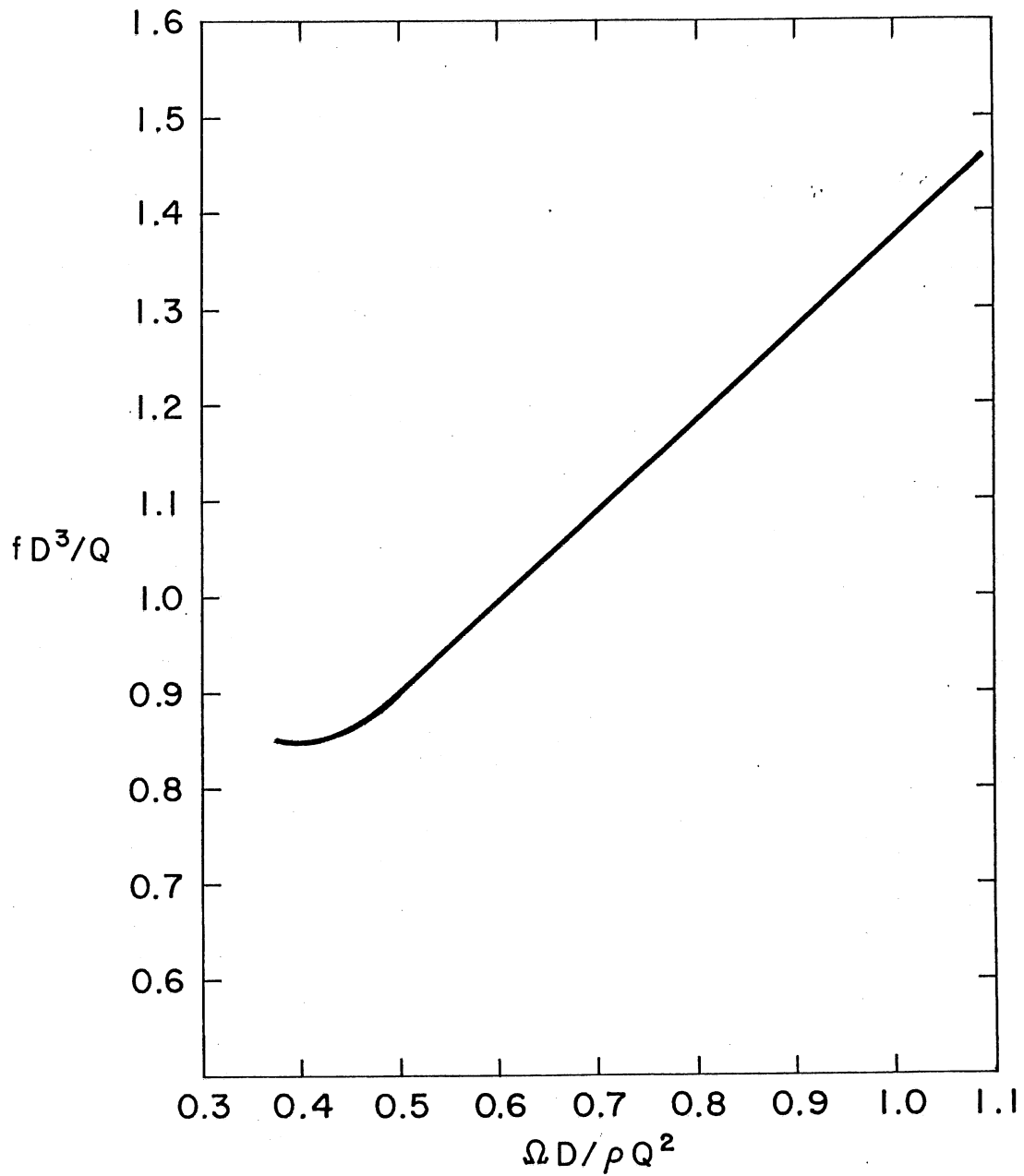


Fig. 30. Surge frequency as a function of momentum parameter for a straight tube. (Adapted from Cassidy and Falvey, 1970.)

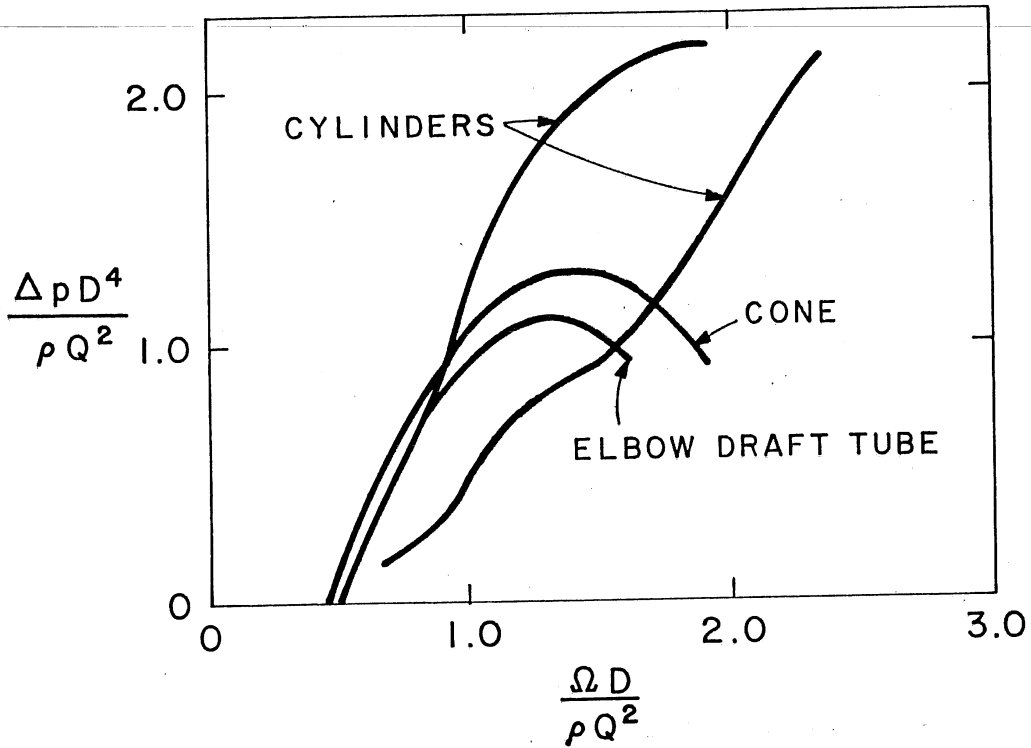


Fig. 31. Amplitude of pressure pulses during surging. (Adapted from Falvey and Cassidy, 1970.)

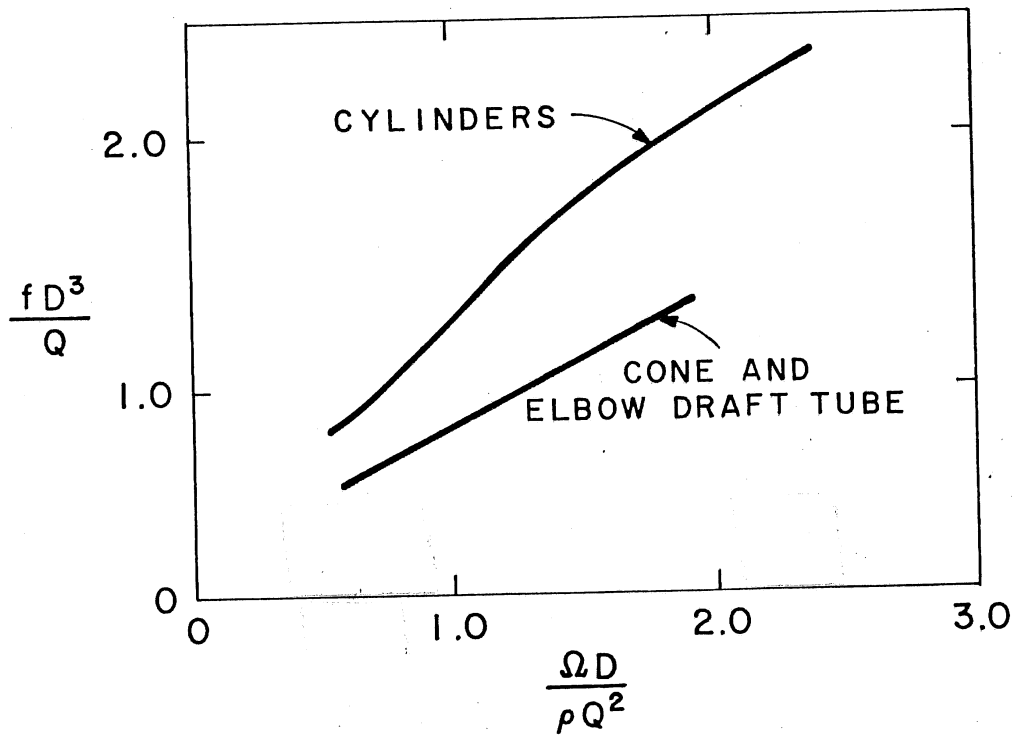


Fig. 32. Surging frequencies for straight cylinders and diffusing passages. (Adapted from Falvey and Cassidy, 1970.)

- (8) Rankine vortex swirl distribution is superior to solid body rotation at moderate cone angles up to about 20° . At higher cone angles the solid body rotation seems to be superior.
- (9) The combination giving the best performance in the shortest diffuser seems to be a diffuser with a 15° cone angle with Rankine vortex swirl profile and moderate swirl angle $\delta = 10^\circ-15^\circ$. The pressure recovery coefficient for $AR = 4$ is about $C_{p_{\alpha\beta}} = 0.75$.
- (10) Several papers dealing with strongly swirling inflow were also reviewed. These papers suggest that for swirl angles larger than $\delta = 25^\circ-38^\circ$ one encounters axial flow reversal, and for $\delta > 50^\circ$ surge sets in diffusers. Increasing the diffuser cone angle tends to weaken the surge.

C. Effect of Wall Jets on Diffuser Flow

Diffuser performance may also be improved by annular injection of higher velocity flow. In this section we shall specifically concentrate on injection of a moderate amount of wall jet flow used to energize boundary layers and to increase their resistance to separation.

A separate topic is the application of injection on the ejector principle. In that case one injects a larger amount of high momentum fluid with the objective to entrain and accelerate the main flow so that the pressure at the draft tube inlet is lowered. The result is an increase in the effective head seen by the turbine; this use of annual injection is discussed e.g. by Moses et al. (1981). The increase in effective head is outside the scope of this report, and so only the use of injection for prevention of flow separation will be reviewed.

The first attempt to study annular injection seems to have been that of Nicoll and Ramaprian (1970). They studied the effect of tangential injection on three diffusers with $2\phi = 10, 20$ and 30° , all with an area ratio of three. The ratio of slot area to inlet area was $c_1 = 0.0455$, and the Reynolds number was 600,000. The results were presented in terms of a pressure coefficient accounting for the additional momentum flux of the injected fluid

$$C_{pr} \equiv \frac{p_2 - p_1 + (p_2 - p_j)c}{\bar{q}_1(1 + ck^2)} \quad (58)$$

where $k \equiv U_j/U_1$, $c \equiv$ jet mass flow/inlet mass flow, and p_j is the static pressure at the jet exit plane. The injection rate was characterized by a ratio defined as

$$\frac{U_j}{U_1^*} = \frac{U_j}{U_1} / (1 + c) \quad (59)$$

Their results, shown in Fig. 33, indicated that the injection improved the performance of the diffusers, the more so for the wider cone angles. The resulting pressure rise was about equal for all three diffusers. The performance was found to be a strong function of the injection velocity, with a maximum near $U_j U_1^* = 1.1$ or $k = 1.16$. The corresponding optimum injection mass flow rate was 5.3 percent of the inlet mass flow.

Fiedler and Gessner (1972) investigated injection in 2-D diffusers. The diffuser had a fixed wall length of $L/W_1 = 4.25$, and the area ratio was varied by changing the spreading angle up to 30° (corresponding to $AR = 3.3$). Reynolds number was set at 90,000. With no jet blowing, the optimum spreading angle for the chosen L/W_1 was $2\phi = 14^\circ$, giving $AR = 2.05$. The results were presented in terms of the coefficients

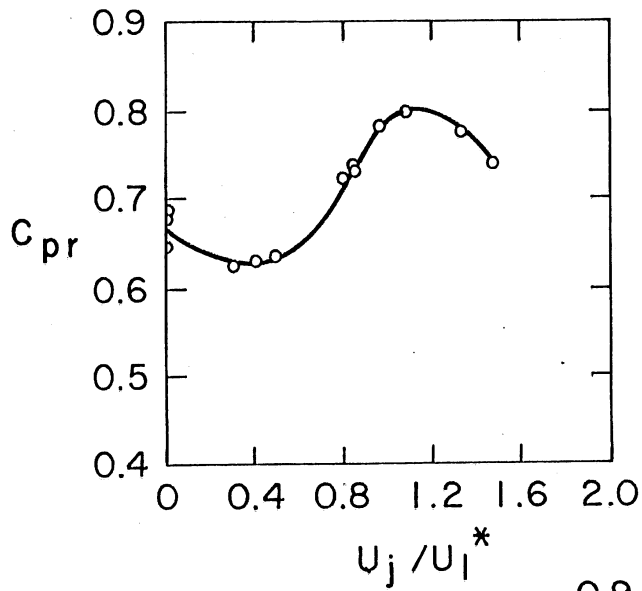
$$C_p = \frac{P_2 - P_1}{q_1} \quad (60)$$

and

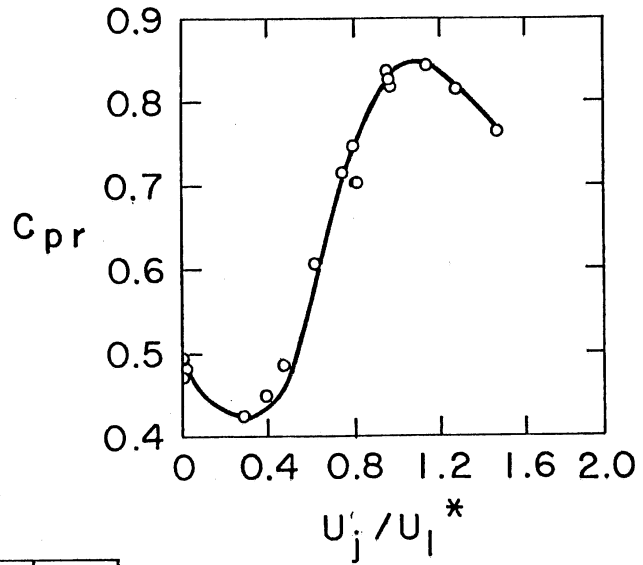
$$C_{p'} = C_p / \left[1 + \frac{c}{\alpha_1 \eta_b} \left(k^2 - \frac{P_2 - P_j}{q_1} \right) \right] \quad (61)$$

where η_b is the efficiency of the blower system, for which they chose a value of 0.6. Their results, plotted against the mass flow ratio $c \equiv c_1 k$, showed that for a given slot C_p increases monotonically with k towards a constant value (Fig. 34). The coefficient $C_{p'}$, which takes into account the power required to supply the jets, reaches a maximum at a value of k which depends on the slot height and, to some degree, on the diffuser angle. For the smallest slot height with $c_1 = 0.02$, the optimum jet velocity was $k \approx 1.9$, giving a mass flow rate $c_1 = 0.038$. For $c_1 = 0.063$ the corresponding values were $k = 1.4$ and $c = 0.088$, and for $c_1 = 0.16$, it was $k = 1.01$ and $c = 0.162$. The observed trend thus was that k is a function of c_1 , being well over one at small slot sizes and decreasing towards unity for large slots. The overall efficiency characterized by $C_{p'}$ was seen to improve monotonically despite the blower losses. Crossplot of the data of Fig. 34, shown in Fig. 35, indicates that the injection provides benefits only at large spreading angles, where the flow is separated in the absence of injection.

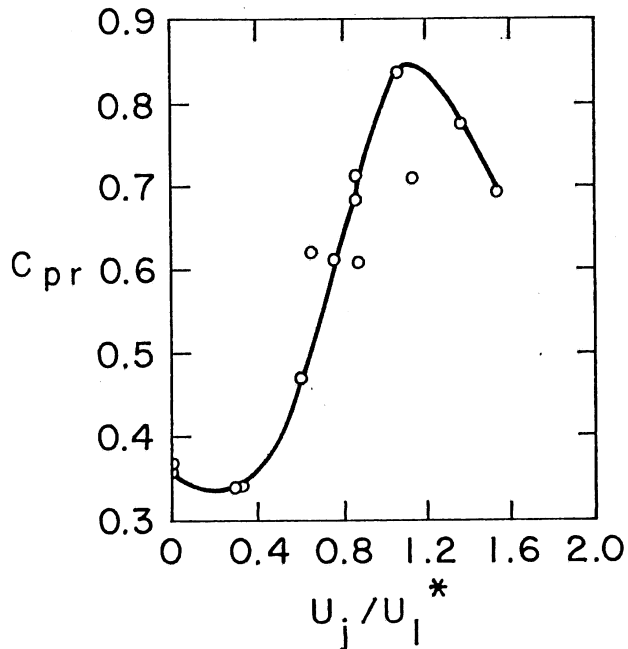
The most comprehensive study is that of Duggins (1975) and Duggins et al. (1978) concerning conical diffusers. Two diffusers with a tailpipe were investigated: both had an area ratio of 3.26 and differed in cone angle, which was $2\phi = 20^\circ$ and 30° , respectively. The annual injection was



a) $2\phi = 10^\circ$

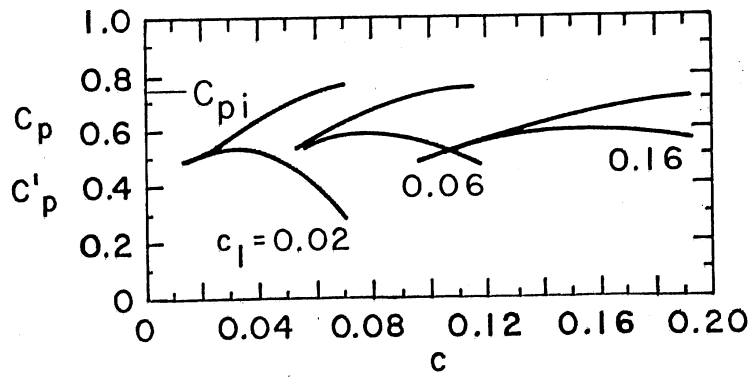


b) $2\phi = 20^\circ$

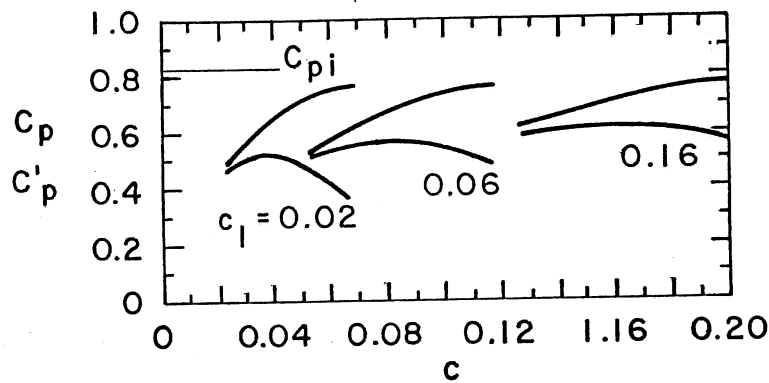


c) $2\phi = 30^\circ$

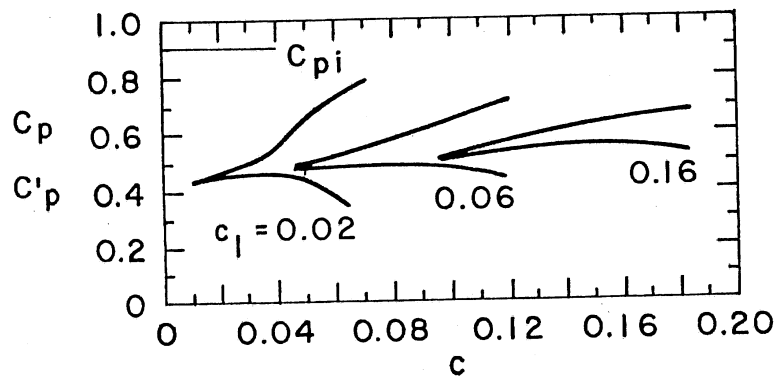
Fig. 33. Effect of wall jet injection velocity on the performance of diffusers with $AR = 3$. (Adapted from Nicoll and Ramaprian, 1970.)



a) $2\phi = 14^\circ$



b) $2\phi = 20^\circ$



c) $2\phi = 30^\circ$

Fig. 34. Effect of wall jet mass flow injection rate on the performance of two-dimensional diffusers with a fixed wall length $L/W_1 = 4.25$. (Adapted from Fiedler and Gessner, 1972.)

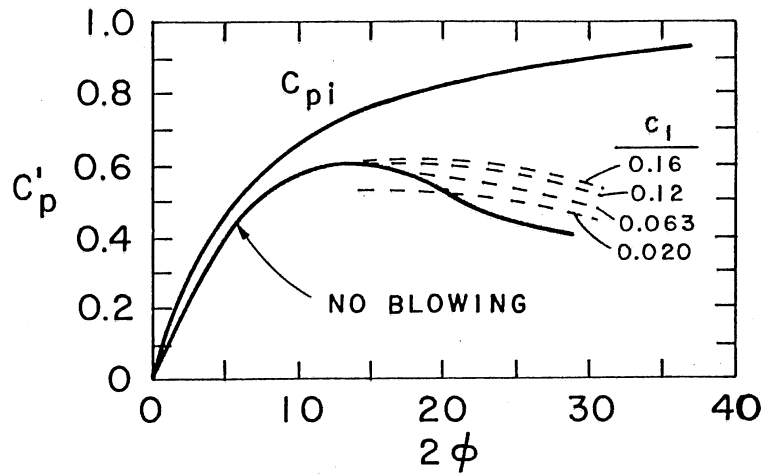


Fig. 35. Effect of slot size on the maximum effective diffuser pressure recovery. (Adapted from Fiedler and Gessner, 1972.)

done in two different ways: axial (parallel to the diffuser axis) and tangential along the wall. The results were presented in the latter of the two papers in terms of

$$C_{pr} = \frac{p_2 - p_1}{\bar{q}_1} \frac{1 + c}{1 + ck^2} \quad (62)$$

where p_2 was measured at the cone exit plane rather than in the tailpipe. A range of slot heights was investigated, a total of seven heights spanning a range $c_1 = 0.032 \div 0.393$. The results for the axial injection are presented in Fig. 36, plotted against three variables: k , c , and the momentum ratio ck . Starting with the top graph, one observes that all slots gave the same C_p when k was optimized, increasing its value from 0.28 to about 0.75. The optimum k was seen to depend on the slot size c_1 . For the smallest slot size, $c_1 = 0.032$, the best velocity ratio k was about two, while for large slots k gradually decreased to a constant value of about 1.1. The middle plot shows that as the slot size goes up, the needed mass flow rate at optimum goes up as well, while no additional benefit is obtained. If one chooses $c \leq 0.1$ as the upper limit on the jet mass flow, one finds this limits the slot area to $c_1 \leq 0.07$. The bottom plot shows a collapse of data for the small slots $c_1 < 0.1$, when plotted against the momentum ratio ck ($\equiv c_1 k^2$). This implies that the performance of small slots depends on the momentum of the injected fluid. It may be seen that at low values of c most of the benefits of injection are obtained by the time $c_1 k^2$ reaches a value of about 0.12. From this it follows that at small c_1 the required k may be related to c_1 by

$$k = 0.35 / \sqrt{c_1} \quad (63)$$

At larger values of $c > 0.1$, the optimum k stabilizes at a constant value of around 1.1. Duggins et al. (1978) also studied tangential injection (Fig. 37), but they found it inferior to axial injection. The two types of injection are compared in Fig. 38, which shows that the tangential injection gives a smaller pressure recovery, and moreover requires a higher flow rate at the optimum point. Among other main results of their study are that for $k < 0.4$ the performance with blowing was worse than without, the worst point being $k = 0.2$. Also, the results for the 20° diffuser showed that the best performance was not better than the 30° diffuser. This implies that once blowing is applied, there is no point in using a shallow angle diffuser. As a final note, one ought to mention that the Duggins data were affected to an unknown degree by the presence of the tailpipe and their results thus should be used with some caution.

Summary of the Wall Jet Effects

Based on the four papers quoted, one can draw the following conclusions:

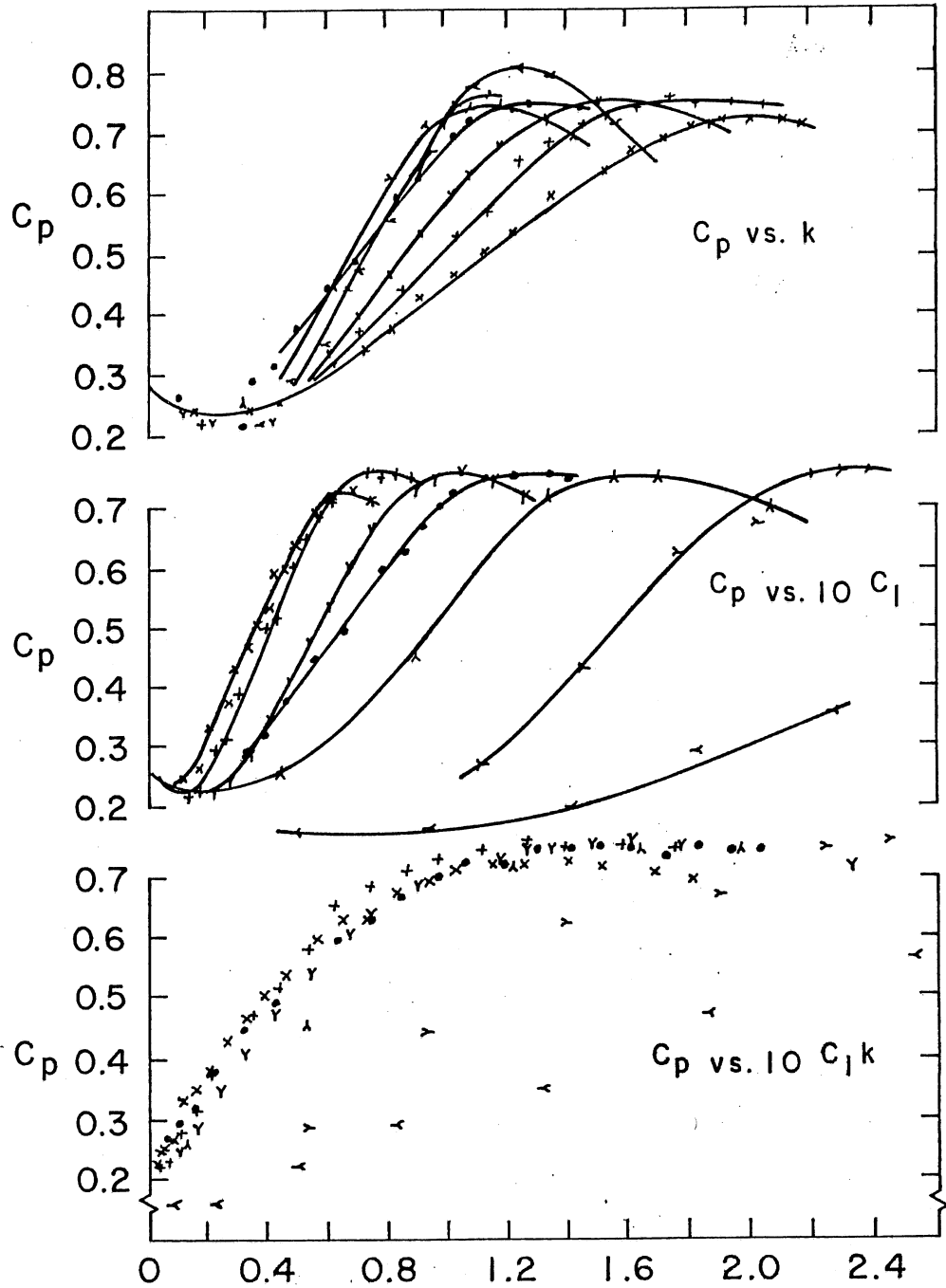


Fig. 36. Effects of wall jet injection velocity, mass flow rate and momentum ratio on pressure recovery coefficient. Axial injection and 30° cone angle. (Adapted from Duggins et al., 1978.)

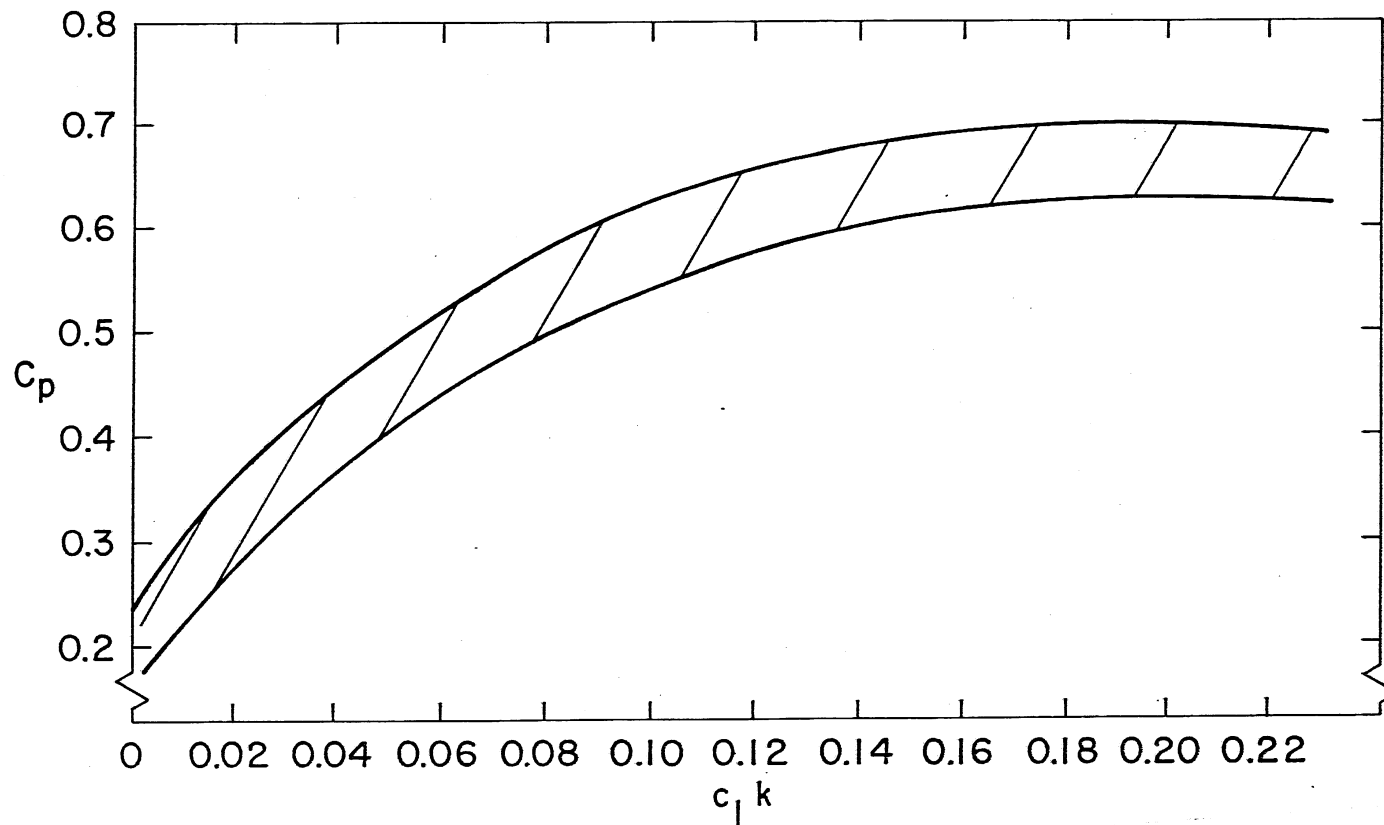


Fig. 37. Effect of momentum ratio on pressure recovery coefficient for tangential injection and 30° cone angle. (Adapted from Duggins et al., 1978.)

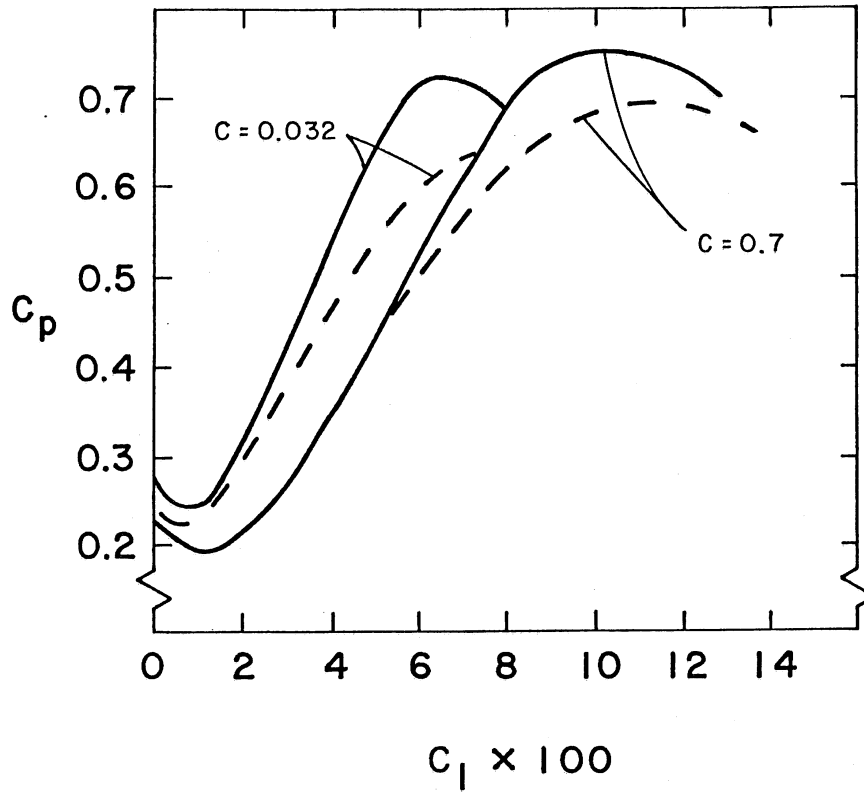


Fig. 38. Comparison of axial and tangential injections for two slot sizes. — axial, --- tangential. (Adapted from Duggins et al., 1978.)

- (1) axial blowing seems preferable to tangential blowing,
- (2) optimum slot area is on the order of 6 percent of the inlet area, with jet velocity on the order of 1.2 times the mean inlet velocity; the resulting jet mass flow ratio is on the order of 7 percent of the inlet flow,
- (3) diffuser cone angle should be greater than 10° if injection is to be useful, and as high as 30° to take the full advantage of blowing, and
- (4) pressure rise obtained with an optimized injection system is as high as 0.8-0.85 times the dynamic pressure based on the mean inlet flow velocity.

D. Other Methods of Increasing Performance of Wide Angle Diffusers

A number of methods have been devised to deal with wide angle diffusers, meaning diffusers with large regions of separation and poor pressure recovery. Some of the techniques for very wide angle diffusers, $2\phi > 25^\circ$, have been found satisfactory in making the exit flow more uniform. Among these belong multiple screens, reviewed in detail by Mehta (1976), stars placed along the centerline (Welsh, 1976) and radial splitter vanes with a trip disk used by Rao (1971) and Rao and Seshadri (1976) to control and steady down (but not eliminate) flow separation. It should be stressed that these techniques are used mainly to make the exit flow uniform, while the resulting pressure recovery is very poor.

For moderately wide diffusers, just above the stall line, proposed methods include distributed suction (Furuya et al., 1966), vortex generators (Senoo and Nishi, 1973) and the use of trapped vortices such as that proposed by Adkins et al (1980).

From the point of view of draft tubes, none of these methods appears satisfactory: most of these methods depend on a device placed in the stream, which would tend to cavitate and/or erode, and the others require suction machinery which would mean increased complexity and tendency to plugging. Because of this, none of these techniques will be reviewed here, but the interested reader may turn to the above references for details.

V. IMPLICATIONS OF DIFFUSER LITERATURE FOR DRAFT TUBE DESIGN

The sketches of draft tubes shown earlier in Fig. 1 illustrate the state-of-the-art in draft tube design for low-head sites. It may be seen that draft tubes have lengths that are typically on the order of four to five times the inlet diameter. Their area ratios are usually close to four, and the resulting effective cone angle is around 13 degrees, which is a fairly high value. Finally, the shape of the draft tube has to conform to a number of constraints dictated by the turbine type and by the installation site. As a result, the draft tubes are rarely conical and their centerlines are often bent. It is clear that the draft tubes are substantially different from the laboratory diffusers discussed in the previous chapter. Therefore, in the following we shall return to the findings of the previous chapter and discuss their implications for practical draft tubes.

Optimum Conical Diffusers

The laboratory experiments have shown that the optimum spreading angle for conical diffusers is around 6° , providing the maximum pressure recovery for area ratios up to five or six. Good pressure recovery is obtained up to $2\phi = 8^\circ$. By contrast, the draft tubes of current hydroplants are more compact and utilize much larger spreading angles (on the order of 13°). In view of Fig. 13, which shows the decrease in pressure recovery with spreading angle, and in view of the fact that the bends usually found in draft tubes tend to degrade performance especially at larger spreading angles, one would expect the typically used draft tubes to have very poor pressure recoveries. That, however, does not seem to be the case. While the use of large spreading angles in draft tubes is mainly the consequence of cost considerations trading off some efficiency versus the extent of required civil works for draft tube construction, the performance of these draft tubes is believed to be fairly high with pressure coefficients quoted to be around 0.75 (Zowski, 1983), although it is not certain what was the definition of the pressure coefficient which led to this value.

The discrepancy in the expected and actual performance levels must be due to the differences between laboratory diffusers and draft tubes. To begin with, there is a substantial difference in Reynolds number, which is 100-300 times larger in draft tubes than in typical experiments; increasing Reynolds number improves boundary layer resistance to separation and thus permits larger spreading angles. Another difference is in the turbulence level of the inlet flow. In laboratory flows the turbulence level is kept low, below one percent. By contrast, the flow leaving the turbine runner is naturally highly turbulent, and turbulence is known to improve the performance of wider-angle diffusers.

Consequently, it appears that the laboratory diffuser studies give conservative values for the maximum spreading angles that one may use in

the highly turbulent, high Reynolds number draft tubes. However, they still provide an understanding and feeling for the trends that one may expect.

Distorted Velocity Profiles

The shape of the inlet profile is also important. Wake-like profiles with velocity maximums near the walls were shown to delay flow separation, and thus permit larger spreading angles and/or higher pressure recoveries. Velocity nonuniformity around 10 - 30 percent were found to be the most beneficial. This suggests a possible strategy for shaping the runner blades or by some other means to produce mild velocity nonuniformities of the desired wake-like shape, without reducing the turbine efficiency.

Bent Draft Tubes

Vertical Kaplan and Francis turbines require 90° bent draft tubes, and bulb turbines require S-shaped tubes. As has been found in basic diffusers and in draft tube research, the pressure recovery in a diffusing passage deteriorates as the bend angle increases. In 90 degree turns the losses are very high, and experience has shown that it is advantageous to flatten the draft tube in the turn so as to reduce the ratio of radius of curvature of the duct height (Mockmore, 1937; Kindsvater and Randolph, 1954). Furthermore, it has been found that it is best to accomplish the required turning at constant area, and recover pressure as much as possible in the straight section ahead of the bend and the rest after the bend. This results in a larger draft tube, however, and a greater cost. Consequently, in low head applications, which typically employ high speed machines and where draft tube cost and performance are important, one should stay away from classical vertical Kaplan turbines in favor of axial flow runners with straight or at most S-shaped draft tubes.

Swirl

It has been observed that a small amount of residual swirl leaving the runner and entering the draft tube improves the draft tube efficiency. For example, Daugherty and Francini, p. 490 (1977), mention that it has been found that the best efficiency is obtained when the turbine blades produce less than complete turning of the flows so that the flow exits with some small angle away from the radial direction. This optimum angle increases with increasing specific speed, i.e. the higher the specific speed, the greater the swirl ratio for optimum system efficiency. Daugherty and Francini quote 15° angle (75° from the runner tip velocity) for high specific speed machines.

This empirical finding agrees with the laboratory results on swirl effects, which indicate that the best performance improvement is obtained for diffusers with cone angles close to 15°, achieved by using a moderately high inlet swirl (swirl angle of 10 - 15°).

The maximum efficiency of the turbine alone, without the draft tube, would be achieved by having the flow exit the machine in the radial direction. Letting the flow exit with some swirl left reduces the turbine

efficiency, the loss hopefully being offset by an increase in draft tube pressure recovery. If the draft tube is poorly designed, or if the constraints of the particular installation are such that the resulting draft tube has flow separation without the swirl, relatively high swirl may be found to be the optimum for the system. Otherwise, it is better to design the draft tube so that it does not need high swirl to keep the flow attached; the efficiency of the system as a whole may then be expected to be higher as less swirl will be discarded at the runner exit.

Wall Jets

As already discussed, injection of wall jets at the draft tube inlet is being considered for performance improvement. The data available in the diffuser literature were shown to indicate substantial gains in pressure recovery. A key question regarding implementation of an injection system is whether its benefits can more than offset the direct loss due to water bypassing the turbine, and being lost to power generation. The power generated may be expressed as

$$\text{Power} = QH \eta_Q \eta_H \quad (64)$$

where η_Q represents the loss of power due to reduction of Q of the bypass

$$\eta_Q = \frac{1}{1 + c} \quad (65)$$

and

$$\begin{aligned} \eta_H &= \eta_{\text{turbine}} - \frac{H_{\text{loss draft}}}{H} \\ &= \eta_{\text{turbine}} - \frac{H_{\text{loss draft}} \text{ k.e.}}{\text{k.e.} H} \end{aligned} \quad (66)$$

where η_{turbine} is the efficiency of the turbine minus the draft tube. Let's take a representative example with $\text{k.e.}/H = 0.4$ and $\eta_{\text{turbine}} = 0.96$, and express the loss in the draft tube as

$$\frac{H_{\text{loss draft}}}{\text{k.e.}} = 1 - C_p \alpha \beta \quad (67)$$

If the draft tube had a relatively mild spreading angle on the order of 10° or less one could expect a pressure recovery coefficient on the order of 0.70. Let us suppose one decides to make the draft tube shorter, for cost or other reasons, so that the pressure recovery coefficient drops to 0.5. Then let us suppose, that by applying an injection system with $c = 0.07$,

we succeed in getting back to the original value of $C_p = 0.7$. What is the overall benefit? The original efficiency is

$$\eta_1 = \eta_Q \eta_H = 1 \times (0.96 - 0.5 \times 0.4) = 0.76$$

and the efficiency of the modified system is

$$\eta_2 = 0.935 \times (0.96 - 0.3 \times 0.4) = 0.785$$

This means that in this example the overall efficiency of the system was increased by 2.5 percentage points, i.e. a little over 3 percent more power would be generated. To determine whether this benefit is worthwhile, one has to weigh this potential efficiency increase, plus savings due to shorter draft tube against the cost of the added injection system and its maintenance.

VI. SOME OBSERVATIONS ON DRAFT TUBE SIZE AND COST

A Note on Hydropower Codes

The codes developed for hydropower applications specify that turbine efficiency is to include performance of the whole turbine/draft-tube assembly. The efficiency is based on net head defined as the difference between the total head at the turbine inlet and the total head at the tailwater level. The total head at the tailwater level includes a velocity head which in the ASME code is based on the tailrace velocity, while the code of the International Electrotechnical Committee (IEC) is based on the average velocity at the draft-tube exit. It may be observed that the velocity head used in the ASME code is typically very small, while the one used in the IEC code can be appreciable. Consequently, the quoted efficiency depends on the code used to calculate it, and the IEC code will always produce a higher value than the ASME code.

The definition used by the IEC code is not meaningful. In fact, it actually provides a loophole: if the turbine manufacturer were to use a short constant area duct (instead of a diffusing duct) for a draft tube, the calculated efficiency would increase as losses in the draft tube due to skin friction and insufficient diffusion would be minimized. Of course, the actual power output would be reduced, and so the real efficiency would be lower. From the point of view of the purchaser, such a definition of efficiency is not useful.

To minimize this problem some national codes set a minimum requirement for the draft tube area ratio, e.g. the Swiss code sets it at a minimum of three (Zowski, 1983). In some South American countries the requirements are stated in terms of the maximum permissible ratio of exit kinetic energy to the net head (Zowski, 1983). Such constraint was also proposed by Hunt (1959) and Purdy (1979) who suggested that the exit kinetic energy should be at most one percent of the available head. Elsewhere, the codes tend to leave the responsibility of specifying the draft tube exit area to the purchasers, who often exercise their right by prescribing the maximum permissible exit velocity. In this context a velocity on the order of 3 m/sec is often specified (Zowski, 1983).

Draft Tube Area Ratio

Some idea about the magnitude of the velocity at the draft tube inlet of Kaplan turbines may be gained from the survey of de Siervo and de Leva (1977), which provides the dimensional velocity at the draft tube inlet (Fig. 39). This velocity is seen to span the range 5.5 - 14.5 m/sec, with the mean value around 9 m/sec and slowly decreasing with specific speed. Taking a draft tube area ratio in the commonly used range of 3 to 4 will bring the exit velocity for most of the quoted installation below 3 m/sec, i.e., below the value that is apparently found to be acceptable by some.

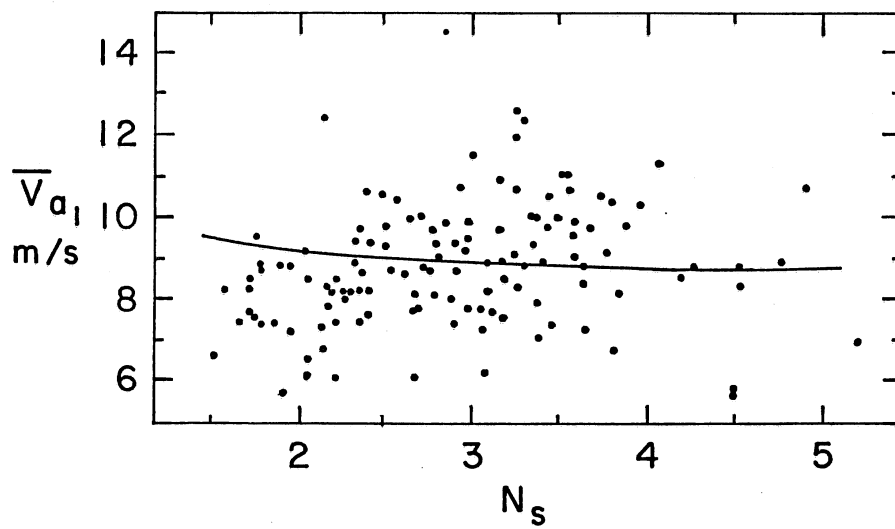


Fig. 39. Water velocity at draft tube inlet for Kaplan turbines. (Adapted from de Siervo and de Leva, 1978.)

However, the quoted limit of 3 m/sec is not a particularly sound value. It represents a head of 0.45 m, which is a significant portion of the gross head of many low-head hydroplants.

If one accepts the suggested requirement that the kinetic energy of the draft tube exit flow (based on the mean velocity) should not be more than one percent of the available head, one may ask what implications does this have for the draft tube area ratio. Starting from Eq. (10) we have

$$\frac{\frac{v_a^2}{2gH}}{AR^2} = \frac{1}{AR^2} \frac{v_a^2}{2gH} = 0.0169 N_s^2 / AR^2 < 0.01$$

i.e.

$$\boxed{AR > 1.3 N_s} \quad (68)$$

It should be realized that choosing the area ratio according to Eq. (68) will not necessarily lead to the most efficient system. It merely guarantees that the minimum kinetic energy at the draft tube exit will be at most one percent of the total head. The actual kinetic energy lost at the exit could be substantially (several times) higher than that. Also the maximum practical value of AR is about 5, because any increase beyond this area ratio is known to bring no additional benefits in pressure recovery (at least for the lower Reynolds number laboratory diffusers). This limits the applicability of Eq. (68) to

$$N_s < 3.8 \quad (69)$$

The only positive result guaranteed to the purchaser by the one percent requirement is that it limits the velocity head adjustment allowed by the IEC code to one percent of the net head, which makes the definition of the efficiency more meaningful. On the other hand, there is a possible drawback. For very high speed machines the one percent constraint could force the manufacturer to build a draft tube with an area ratio greater than five, i.e. beyond the optimum. The additional cost of construction of the draft tube would be completely wasted, as no increase in plant efficiency would result. A better approach to the problem of maximizing the overall efficiency, than specifying the maximum kinetic energy at the exit, would be to do away with the velocity head adjustment to the net head. The quoted efficiency would then have a real meaning, and the optimization of the total system efficiency and of the total cost could be left to the manufacturer.

Trends of Draft Tube Size with Specific Speed

In the following we shall make an estimate of the total volume of the draft tube structure and inquire into its dependence on the specific speed.

Let us consider a conical draft tube with inlet diameter D_1 , exit diameter of D_2 and length L . The volume of the structure may be estimated either as a shell, relevant to the amount of material needed, and as the enclosed volume, relevant to cost of excavations.

$$V_{\text{shell}} \approx 1/4 \pi (D_1 + D_2)(t_1 + t_2)L \quad (70)$$

where t is the thickness of the shell wall. Assuming that the wall thickness is proportional to the local diameter, we can write

$$V_{\text{shell}} = \frac{1}{4} \pi \frac{t_1}{D_1} \times \left(1 + \frac{D_2}{D_1}\right)^2 \frac{L}{D_1} D_1^3 \quad (71)$$

i.e. the volume goes up slowly with area ratio, linearly with L/D_1 and cubically with D_1 . For the enclosed volume we write

$$V_{\text{encl}} = \frac{\pi}{8} \left(1 + \frac{4t_1}{D_1}\right) \times \left[1 + \left(\frac{D_2}{D_1}\right)^2\right] \frac{L}{D_1} D_1^3 \quad (72)$$

which has a similar dependence as V_{shell} .

Since for a given H , runner exit velocity, according to Eq. (10), increases linearly with specific speed, the draft tube inlet area decreases in an inverse proportion and

$$D_1 \sim N_s^{-1/2} \quad (73)$$

If we consider the case where the area ratio of the draft tube and its spreading angle are fixed at some near-optimum value (say $AR = 5$, $2\phi = 12^\circ$) regardless of the kinetic energy ($k.e./H$) at the inlet, then we have

$$V_{\text{shell}} \sim V_{\text{encl}} \sim N_s^{-1.5}$$

i.e. the increase in the specific speed leads to a substantial reduction in draft tube size.

On the other end of the spectrum of options one could require that the area ratio increases with increasing N_s to satisfy the one-percent requirement for the kinetic energy at the draft tube exit. Restricting our attention to axial machines and to the specific speed range of 1.5 to 3.8, we have by Eq. (68) a relation between the area ratio and the specific speed

$$\left(\frac{D_2}{D_1}\right)^2 = 1.3 N_s \quad (74)$$

Considering fixed-spreading-angle cones, we can write

$$\frac{L}{D_1} = \frac{1}{2 \tan \phi} \left(\frac{D_2}{D_1} - 1\right) \approx \frac{(D_2/D_1)^2}{8 \tan \phi} \quad (75)$$

where the last approximation is quite accurate for D_2/D_1 between 1.6 and 2.6. Substituting Eqs. (73), (74), and (75) into Eqs. (71) and (72) we obtain

$$V_{\text{shell}} \sim (1 + \sqrt{1.3 N_s})^2 N_s^{-1/2} \quad (76a)$$

$$V_{\text{encl}} \sim (1 + 1.3 N_s) N_s^{-1/2} \quad (76b)$$

Substituting for N_s we find that both volumes increase with N_s to a small power

$$V_{\text{shell}} \sim N_s^{0.14} \quad (77a)$$

$$V_{\text{encl}} \sim N_s^{0.26} \quad (77b)$$

Thus, we arrive at the conclusion that if we desire to maintain a fixed ratio of exit kinetic energy to net head, increasing specific speed actually increases the draft-tube size. This somewhat surprising result may be explained by the following argument. For a given head and a volume flow, there is one draft-tube exit area for which the average exit kinetic energy equals a given fraction of the head. Increasing N_s means a smaller D_1 , and if ϕ is fixed, this requires an addition of a new section of the draft tube inlet side, connecting it to the smaller diameter. It is this added section which is responsible for the increase evident from Eq. (77).

VII. SUMMARY AND RECOMMENDATIONS

A. Summary

Increasing the specific speed of turbomachines used for low head hydropower brings advantages in reducing the size of the machines or in permitting the use of a smaller number of turbines at a given site. As the specific speed increases, so does the kinetic energy of the water exiting the runner. The fraction of the head exiting in the form of the kinetic energy increases approximately as the square of the specific speed. This fraction is small for $N_s < 1$, but it becomes important around $N_s = 1.5$ and at $N_s = 4$ some forty percent of the head is in the form of kinetic energy at the runner exit. This kinetic energy is responsible for the observed rapid decrease in turbine efficiency at high specific speeds.

A large part of the kinetic energy is recovered in the draft tube, where it is converted into additional potential energy acting across the turbine; nevertheless some 25 or more percent of the kinetic energy ends up a loss, the exact amount depending on the draft tube efficiency. The draft tube has a special importance in low-head hydropower. In low-head high-specific-speed applications the draft tube constitutes an important part of construction costs because of its size relative to the rest of the structure, and due to the need for excavations needed to prevent cavitation. On the performance side, the draft tube's importance comes from its key role in assuring high overall efficiency; an improvement in draft tube pressure coefficient by 0.1 translates into a four percent improvement in the overall efficiency at $N_s = 4$!

In order to minimize the amount of kinetic energy lost to the tailrace, it is often suggested that one should use a draft tube area ratio such that the kinetic energy based on the average velocity at the draft tube exit is less than one percent of the head. This requirement is not too meaningful because it prescribes a draft tube area ratio which is approximately linearly proportional to the specific speed, while the optimum area ratio is around four to five. This means that at low specific speeds this requirement leads to too small AR (at $N_s = 1.5$ it gives $AR \approx 2$), while for $N_s > 3.8$ it leads to excessively large AR, beyond the point where an area ratio increase provides any benefits ($AR = 5$).

Increasing specific speed of turbomachines is known to increase strongly their tendency to cavitation. One reason for this increase is the lowering of pressure at the runner exit due to the high speed of the exiting flow. At $N_s = 4$ some 30-35 percent of the cavitation index (Thoma's sigma) is due to this effect. The result is a requirement to install the machine low enough to prevent cavitation, and this frequently means a substantial amount of excavation work.

Experience acquired in laboratory diffuser experiments, and supported in many instances by draft tube experience, indicates that diffuser

performance may be augmented by several means all of which tend to strengthen the resistance of boundary layers to separation:

- (1) High levels of turbulence in the inlet flow tend to promote transverse momentum transfer to the boundary layers increasing resistance to separation. Turbomachinery flows are naturally highly turbulent and this should aid pressure recovery.
- (2) Axial velocity distortions with velocity overshoot near walls, again strengthening the boundary layers. Optimum overshoots are quite moderate (10-15 percent).
- (3) Addition of swirl provides velocity overshoot near the walls and in addition enhances turbulence generation. Best results are obtained with moderate swirl angles (10° - 15°), while large swirl angles ($> 30^{\circ}$) can lead to instability and surging.
- (4) Injection of wall jets energizing the boundary layers can also be very effective, although the jet flow bypassing the turbine is lost to power generation. Optimum values for wall jet injections are near seven percent mass flow ratio (jet flow/main flow) with jet velocity at 1.2 times that of the main flow.

All of these means are most effective at larger cone angles ($2\phi = 15^{\circ}$ - 25°) and in fact, one of their effects is to move the optimum spreading angle to higher values. Regular diffusers with uniform flow at the entry give the best performance with $AR = 0(5)$ and $2\phi = 5^{\circ}$. As we have seen the performance of laboratory diffusers drops off fairly rapidly with increasing cone angle, but typical draft tubes have much higher Reynolds numbers, and the performance curve with respect to (2ϕ) may be expected to be more flat. For them the cost/benefit consideration will lead to spreading angles much larger than 5° . Draft tubes with $AR = 4-5$ and $2\phi = 10^{\circ}$ are probably near optimum. If a shorter draft tube has to be used, i.e. larger spreading angle, one may consider different strategies involving swirl and mean velocity profile distortions to maintain the pressure recovery levels at acceptable levels. For even shorter draft tubes where such methods are not sufficient to produce attached flow, one should consider the use of wall jets. As shown in an example in the text, the use of wall jets under such conditions might provide an improvement in overall efficiency even when the loss of power due to water bypass is accounted for. A side benefit of the wall jets under such conditions would be an improvement in flow stability in the draft tube and in the system as a whole.

One special feature of turbomachine diffusers is that they often are bent. The laboratory literature indicates that mild bends with total angles up to 30° have only a small effect on the flow, but beyond that point the performance increasingly suffers. It is advisable to avoid excessive turns by using horizontally placed machines requiring only small bends. For larger turns one should follow the design ideas proposed by Sagi and Johnston (1967) and in general keep the radius of curvature as large as practicable.

B. Recommendations for Further Work

The increasing losses incurred at high specific speeds show that the design of highly efficient draft tubes is essential if even higher specific speed operation is to be economically feasible. There is a need for efficient compact draft tubes to be used in such applications. A review of literature shows that there are large gaps in knowledge about draft tube flows, and it follows that there is a need for a wide-ranging experimental program, with the objective to advance the state-of-the-art in the design of efficient draft tubes. The large amount of work done to date on laboratory diffusers provides an excellent starting point. The data obtained in these studies are not directly applicable to draft tubes on account of the many differences such as in Reynolds number, turbulence level, initial profiles and geometry (all of the laboratory work has been on simple 2-D and axisymmetric diffusers). However, these papers are still very useful as they suggest a number of potentially profitable directions, but these ideas have to be applied to, and proven for, typical draft tube configurations.

Based on the material presented here one can identify a number of investigations that such an experimental program should cover, and these are briefly described below.

Performance of Today's Draft Tubes. The starting point ought to be a study of the performance of current draft tubes. First, one needs to define the most appropriate parameter for measuring the draft tube efficiency. For this, the definitions presented and discussed in this report might be a starting point. Then a survey of a number of installed draft tubes considered state-of-the-art should be undertaken to determine their performance. It is important to do this to find out whether the draft tubes are as good as is being believed and also to establish a benchmark for further work.

Conditions at Draft Tube Inlet. The objective would be to study the conditions existing at the draft tube entry downstream of an actual water turbine. This would include axial and tangential velocity profiles and turbulence intensity. Also of interest is the behavior of these parameters at off-design conditions for fully adjustable and partially-adjustable machines.

Optimum High Reynolds Number Diffusers. The laboratory data show that the optimum results are obtained with area ratio around five and $2\phi \approx 5-6^\circ$. The pressure recovery is known to decrease rapidly with increasing spreading angle. One expects that the curve of pressure recovery would decay much less rapidly in diffusers with Reynolds numbers and turbulence levels typical of water turbine flows. A study should be made of this important point essential to understanding of draft tube performance.

Optimum Swirl. Extend the work done on laboratory diffusers to draft tubes with and without bends. The objective is to establish the optimum swirl angle under a variety of conditions.

Distorted Inlet Profile. Study of possibility of shaping the runner blades so as to produce a prescribed non-uniformity of the axial velocity

profile at the draft tube entry. A wake-like non-uniformity was shown to be highly beneficial.

Bends. Much work needs to be done in the area of bends and their effect on draft tube performance. The available literature deals with low Reynolds numbers and needs to be extended.

Wall Jets. The application of wall jets is a topic that has a special importance to situations where a current draft tube is known to have flow separation, very low efficiency and produces flow instability. It should be also considered whenever there is a need for an efficient highly-compact draft tube.

Definition of Turbine/Draft Tube Efficiency. This topic is a conceptual study aimed at elucidation of the concept of turbine efficiency, and at reevaluation of the definitions used in various codes. It appears that currently used efficiencies do not always convey the information most relevant to economic evaluation of a proposed turbine installation.

ACKNOWLEDGEMENT

The author wishes to acknowledge the many contribution of Dr. R. E. A. Arndt who suggested this study, set the initial directions, and provided much needed help along the way.

REFERENCES

1. Acrivlellis, M. (1977). "Experimental Untersuchungen des Druckrueckgewinns in Kegel-und Carnotdiffusoren bei Drallbehafteter Stroemung," Forch. Ing.-Wes., Vol. 43, No. 4, pp. 126-130.
2. Adkins, R. C., Matharu, D. S., and Yost, J. O. (1980). "The hybrid diffuser," ASME Paper 80-GT-136.
3. Arndt, R.E.A., Farell, C., and Wetzel, J. M. (1983). "Hydraulic turbines," Chapter 6 in Small Hydropower Systems Design, McGraw-Hill.
4. Bradshaw, P. (1963). "Performance of a diffuser with fully-developed pipe flow at entry," Jour. of the Royal Aeronautical Society, Vol. 67, Nov., p. 733.
5. Carson, J. L. and Samuelson, R. S. (1978). "Low head turbines draw attention," Power, Mar., pp. 54-57.
6. Cassidy, J. J. (1969). "Experimental Study and Analysis of Draft-tube Surging," U. S. Bureau of Reclamation, Report REC-OCE-69-5, No. HYD-591, Oct., 1969.
7. Cassidy, J. J. and Falvey, H. T. (1970). "Observations of unsteady flow arising after vortex breakdown," Jour. of Fluid Mechanics, Vol. 41, Part 4, pp. 727-736.
8. Cockrell, D. J. (1964). "Pressure coefficient and diffuser efficiency," Jour. of the Royal Aeronautical Society, Vol. 68, Dec., pp. 844-845.
9. Cockrell, D. J. and Markland, E. (1963). "A review of incompressible diffuser flow," Aircraft Engineering, October, pp. 286-292.
10. Daugherty, R. L. and Francini, J. B. (1977). Fluid Mechanics with Engineering Applications, McGraw-Hill, 1977.
11. Duggins, R. K. (1975). "Conical diffusers with annular injection," Jour. of Mechanical Engineering Science, Vol. 17, No. 4, pp. 237-239.
12. Duggins, R. K., Lampard, D., and Sanders, A. T. (1978). "Further Investigation of Conical Diffusers with Annular Injection," Jour. of Mechanical Engineering Science, Vol. 20, No. 1, pp. 58-64.
13. Falvey, H. T. (1971). "Draft tube surges--A review of present knowledge and an annotated bibliography," U.S. Bureau of Reclamation, Report REC-ERC-71-42, December.

14. Falvey, H. T. and Cassidy, J. J. (1970). "Frequency and amplitude of pressure surges generated by swirling flow," Transactions of IAHR Symposium, Part 1, Stockholm, pp. 1-11.
15. Fiedler, R. A. and Gessner, F. B. (1972). "Influence of tangential fluid injection on the performance of two-dimensional diffusers," ASME, Jour. of Basic Engineering, September, pp. 666-674.
16. Fox, R. W. and Kline, S. J. (1962). "Flow regimes in curved subsonic diffusers," ASME, Jour. of Basic Engineering, September, pp. 303-316.
17. Furuya, Y., Sato, T., and Kushida, T. (1966). "The loss of flow in the conical diffusers with suction at the entrance," Bulletin of JSME, Vol. 9, No. 33, pp. 131-137.
18. Harvey, J. K. (1962). "Some observations of the vortex breakdown phenomenon," Jour. of Fluid Mechanics, Vol. 14, pp. 585.
19. Hunt, H. J. (1959). "Progress in draft-tube design," Civil Engineering, March, pp. 40-43.
20. Kaiser, K. F. and McDonald, A. T. (1980). "Effect of wake-type non-uniform inlet velocity profiles on first appreciable stall in plane-wall diffuser," ASME, Jour. of Fluids Engineering, September, pp. 283-289.
21. Kindsvater, C. E. and Randolph, Jr., R. R. (1954). "Hydraulic model studies of Martin Dam draft tubes," ASCE, Jour. of Hydraulics Div., Vol. 120, pp. 1399-1419.
22. Klein, A. (1981). "Review: Effects of inlet conditions on conical diffuser performance," ASME, Jour. of Fluids Engineering, Vol. 103, June, pp. 250-257.
23. McDonald, A. T. and Fox, R. W. (1966). "An experimental investigation of incompressible flow in conical diffusers," International Jour. of Mechanical Sciences, Vol. 8, No. 2, pp. 125-139.
24. McDonald, A. T., Fox, R. W. and Van Dewoestine, R. V. (1971). "Effects of swirling inlet flow on pressure recovery in conical diffusers," AIAA Jour., Vol. 9, No. 10, October, pp. 2014-2018.
25. Mehta, R. D. (1976), "The design of wide-angle diffusers," Imperial College, London, I. C. Aero Report 76-03, June.
26. Mockmore, C. A. (1938). "Flow characteristics in elbow draft tubes," ASCE, Jour. of Hydraulics Div., Vol. 103, pp. 402-464.
27. Moses, H. L., Myatt, L. and Haynes, W. (1981). "Conical diffusers with peripheral wall jets for low-head hydroelectric systems," Proceedings of Water Power '81, Vol. II, June 22-24, 1981, Washington, D. C., pp. 1292-1307.

28. Neve, R. S. and Thakker, A. (1981). "The effect of superimposed Rankine and forced vortices on conical diffuser performance," Aeronautical Jour., June, pp. 234-239.
29. Neve, R. S. and Wirasinghe, N.E.A. (1978). "Changes in conical diffuser performance by swirl addition," The Aeronautical Quarterly, August, pp. 131-143.
30. Nicoll, W. B. and Ramaprian, B. R. (1970). "Performance of conical diffusers with annular injection at inlet," ASME, Jour. of Basic Engineering, December, pp. 827-835.
31. Palde, U. J. (1972). "Influence of draft tube shape on surging characteristics of reaction turbines," U. S. Bureau of Reclamation, Report REC-ERC-72-24, July.
32. Purdy, C. C. (1979). "Energy losses at draft tube exits and in penstocks," Water Power and Dam Construction, October.
33. Rao, D. M. (1971). "A method of flow stabilization with high pressure recovery in short conical diffusers," Aeronautical Jour., May, pp. 336-339.
34. Rao, D. M. and Seshadri, S. N. (1976). "Application of radial splitters for improved wide-angle diffuser performance in a blowdown tunnel," Jour. of Aircraft, Vol. 13, No. 7, pp. 538-540.
35. Sagi, C. J. and Johnston, J. P. (1967). "The design and performance of two-dimensional, curved diffusers," ASME, Jour. of Basic Engineering, December, pp. 715-731.
36. Senoo, Y., Kawaguchi, N. and Nagata, T. (1978). "Swirl flow in conical diffusers," Bulletin of the JSME, Vol. 21, No. 151, January, pp. 112-119.
37. Senoo, Y. and Nishi, M. (1974). "Improvement of the Performance of Conical Diffusers by Vortex Generators," ASME, Jour. of Fluids Engineering, Vol. 96, No. 1, March, 1974, pp. 4-10.
38. Schiebeler, W. (1955). "Luftstroemungen mit Drall im Kreisrohr hinter Radialem Leitapparat," Mitt. Max-Planck-Institut fuer Stroemungsforschung, Goettingen, Nr. 12.
39. Shaalan, M.R.A. and Shabaka, I.M.M. (1975). "An experimental investigation of the swirling-flow performance of an annular diffuser at low speed," ASME Paper 75-WA/FE-17.
40. Shárán, V. K. (1972). "Improving diffuser performance by artificial means," AIAA Jour., Vol. 10, No. 8, August, pp. 1105-1106.
41. de Siervo, F. and de Leva, F. (1976). "Modern trends in selecting and designing Francis turbines," Water Power and Dam Construction, August, pp. 28-35.

42. de Siervo, F. and de Leva, F. (1977). "Modern trends in selecting and designing Kaplan turbines - Part I," Water Power and Dam Construction, December, pp. 51-56.
43. de Siervo F. and de Leva F. (1978). "Modern trends in selecting and designing Kaplan turbines - Part II," Water Power and Dam Construction, January, pp. 52-58.
44. So, K. L. (1967). "Vortex phenomena in a conical diffuser," AIAA Jour., Vol. 5, No. 6, pp. 1072-1078.
45. Sovran, G. and Klomp, E. D. (1965). "Experimentally determined optimum geometries for rectilinear diffusers with rectangular, conical or annular cross-section," Fluid Mechanics of Internal Flow, Ed. G. Sovran, Elsevier, 1967, pp. 270-319.
46. Squire, H. B. (1960). "Analysis of the vortex breakdown phenomenon," Imperial College, London, I.C. Aero Report 102.
47. Waitman, B. A., Reneau, L. R. and Kline, S. J. (1961). "Effects of inlet conditions on performance of two-dimensional subsonic diffusers," ASME, Jour. of Basic Engineering, September, pp. 349-360.
48. Welsh, M. C. (1976). "Flow control in wide-angled conical diffusers," ASME, Jour. of Fluids Engineering, December, pp. 728-735.
49. Wolf, S. and Johnston, J. P. (1969). "Effects of non-uniform inlet velocity profiles on flow regimes and performance in two-dimensional diffusers," ASME, Jour. of Basic Engineering, September, pp. 462-474.
50. Zowski, T. (1983). Harza Engineering, Chicago, Ill., private communication.